COHERENT PRODUCTION OF PARTICLES IN HADRON--NUCLEUS SCATTERING (EXPERIMENTAL)

By H. H. Bingham

Physics Department, University of California, Berkeley*

(*Presented at the XIth Cracow School of Theoretical Physics, Zakopane, June 8–22, 1971*)

We review data on coherent production reactions from nuclei in π, K, nucleon and antinucleon beams of momenta above ~ 2 GeV/c. Characteristics of the dominant ("vacuum exchange") reactions and rarer ("ω exchange") reactions are summarized.

1. Introduction

Coherent production reactions are yielding new information on total cross-sections for interactions of unstable particles with nucleons, on nuclear radii and shape parameters, on quantum numbers of the produced states and on exchange mechanisms for the production of states of known quantum numbers. It may be possible soon to use information from coherent reactions to estimate scattering amplitudes (and phases) of unstable particles, transition amplitudes from one unstable particle to another as well as further nuclear structure parameters.

Although a full understanding of coherent production reactions ("CPR") will almost surely require understanding of most of the domain of strong and electromagnetic interaction physics, the data available today on these reactions can be explained using only a finite set of ideas. Many of these ideas developed to handle particle interactions with structured targets (nuclei) are finding wider applications, *e. g.* to parton and quark model analyses of the interactions of elementary particles in general (see Jackson's review [2] for a discussion of some of these analogies).

In these lectures I will briefly review some of the gross features expected for CPR's on the basis of some simple kinematical relations, nuclear form factor effects, and rotational invariance. Then I will briefly recapitulate some of the available experimental data reviewed in my talk last year at the Trieste conference [1] and discuss what new data has come in since then. See Professor Goldhaber's talks in these proceedings for the current state of the theory, and Professor Białas' discussion of an exciting revival of some older approaches with a new twist.

* Address: Physics Department, University of California, Berkeley, California 94720, USA.

Other recent theory reviews are by Margolis [3], Glauber [4], Stodolsky [5], Trefil [6] and Fournier [7], and experimental ones by Bellini [8], Franzini [9], di Lella [10], Czyżewski [11], Veillet [12] and Fisher [13]. For reviews of related topics not covered here see: (photoproduction) Ting [14], Leith [15], Silverman [16], Diebold [17] and Lohrmann [18]; (coherent elastic scattering) Bellini [19], Bertocchi [20], Glauber [4]; (K^0 regeneration) Lee and Wu [21], Gilman [22] and recent conference proceedings [23]; (incoherent production reactions) Margolis [3], Fournier [7], Glauber [4], Gottfried and Yennie [24]. For properties of the particles cited see the "Wallet card" [25].

2. *Kinematics*

In the coherent production reaction

$$b+T\rightarrow s+R \tag{1}$$

b is the beam particle, T the target nucleus, R the recoil nucleus (normally in the same state as T, *i. e.* the ground state) and s is the state coherently produced. For CPR, the 4-momentum transfer squared

$$t = (s-b)^2 = (R-T)^2 \tag{2}$$

(where the particle symbols now represent energy-momentum 4-vectors) is restricted by the nuclear form factor to small values and reduces approximately to

$$-t \approx q^2 = q_{||}^2+q_{\perp}^2 \approx -t_{\min}+q_{\perp}^2 \tag{3}$$

where q is the (small) three-momentum of the recoil nucleus (assumed non-relativistic) in the lab system ("LS"), $q_{||}$ and $q_{\perp}$ are its components respectively parallel and perpendicular to the beam direction

$$-t_{\min} = (s-b)^2_{\min} = M_s^2-M_b^2-2q_{||}p_b+2(E_R-M_T)E_b \approx q_{||}^2 \approx \left(\frac{M_s^2-M_b^2}{2p_b}\right)^2 \tag{4}$$

is the minimum momentum transfer required to produce an outgoing system of mass M_s from a beam of 3-momentum p_b, energy E_b, mass M_b. E_R is the recoil energy and M_T the target mass. For coherent elastic scattering $s^2 = b^2$, $t_{\min} = 0$. For CPR where $s^2 \neq b^2$ it is convenient to define

$$t' = |t-t_{\min}| = 2p_bp_s(1-\cos\theta_s) \approx \frac{p_b}{p_s}q_{\perp}^2 \approx q_{\perp}^2 \tag{5}$$

where θ_s is the angle between the outgoing ($\boldsymbol{p}_s$) and the beam ($\boldsymbol{p}_b$) momentum directions in the LS.

3. *Characteristics of coherent reactions*

In order for reaction (1) to be coherent over the nucleus, *i. e.* in order for the amplitudes for the process $b\rightarrow s$ to add coherently from the various parts of the nucleus (nucleons), the transition $b\rightarrow s$ must not "mark" the nucleon on which it took place, *i. e.*

the transition $b \to s$ must not leave information in the residual nucleus which could in principle be used to determine which nucleon was struck. This fundamental condition for coherence leads to some selection rules which are discussed below.

For reactions $b \to s$ of practical interest (*e. g.* $\pi \to A_1$, $K \to Q$), the beam momentum p_b is high enough that the corresponding wavelength

$$\lambda(\text{fermis}) = \frac{2\pi\hbar}{p_b} \approx \frac{1}{5p_b(\text{GeV}/c)} \ll 1\text{fm} \tag{6}$$

i. e. λ is much less than the range of nuclear forces (at least the transverse range), the internucleon distance in the nucleus and thus of course than the radius $1.12\,A^{1/3}$ in fermis. Note that p_b is then much greater than the Fermi momentum of nucleons in the nucleus. Thus no nuclear rearrangement has time to take place in the neighbourhood of b or s during their passage and the coherent production reaction can be described analogously to electron scattering from a crystal, or light diffracting from an extended structure of scatterers. As in these cases, then, we can expect the angular distribution of the outgoing state s to be determined principally by the Fourier transform of $\varrho(\boldsymbol{r})$ the spatial distribution of nucleons in the nucleus, *i. e.* by the nuclear form factor $F(\boldsymbol{q})$

$$F(\boldsymbol{q}) = \int d^3r e^{i\boldsymbol{q}\cdot\boldsymbol{r}} \varrho(\boldsymbol{r}).$$

Because nuclei are approximately spherical with diffuse outer regions, *i.e.* can be described approximately by a density function which is Gaussian in x, y, z, the nuclear form factor is approximately Gaussian in q_x, q_y, q_z or approximately exponential in $t \approx -(q_x^2 + q_y^2 + q_z^2)$

$$|F(\boldsymbol{q})|^2 \sim e^{Bt} \tag{7}$$

where B is the "slope at small t" of the momentum transfer distribution.

$$B(\text{GeV}/c)^{-2} = \frac{\langle r^2 \rangle}{3} = 8.6\langle r^2 \rangle \text{ fm}^2 \approx 11A^{2/3}(\text{GeV}/c)^{-2} \tag{8}$$

where $\sqrt{\langle r^2 \rangle}$ is the rms radius of the nuclear density distribution $\varrho(\boldsymbol{r})$. For carbon $B \approx$ $\approx 60\,(\text{GeV}/c)^{-2}$, for lead ≈ 380. The observed slopes are usually somewhat greater because of absorption effects, however.

The momentum transfer distribution will normally contain factors other than (7), of course, particularly approximately the shape of the t distribution for the corresponding reaction from a free nucleon. For most coherent reactions, *e.g.* those which can proceed *via* vacuum exchange, this t distribution is also exponential with slope characteristic of scattering from a source the size of a single nucleon: $B \approx 10\,(\text{GeV}/c)^{-2}$.

Most of the intensity of the outgoing s beam will be contained within a cone of half angle θ_s

$$\theta_s \approx \frac{p_\perp}{p_s} \approx \frac{q_\perp}{p_b} \lesssim \frac{\pi/a}{p_b} \approx \frac{0.28A^{-1/3}}{p_b(\text{GeV}/c)} \tag{9}$$

where the characteristic momentum transfer of the nucleus

$$\frac{\pi}{a} = \frac{\pi}{\text{nuclear diameter}} \approx \frac{\pi}{2 \times 1.12 A^{1/3}} \approx 0.28 A^{-1/3} (\text{GeV}/c) \tag{10}$$

is ~ 0.12 GeV/c for carbon, ~ 0.05 GeV/c for lead. For momentum transfers much larger than this, the nuclear form factor falls rapidly, *i.e.* the nucleus is unlikely to hold together in the collision and the coherent cross-section becomes small compared with corresponding $b \to s$ production in incoherent or nuclear break-up reactions. For a neon target, and $p_b = 7$ GeV/c for example, $\theta_s \lesssim 17$ mrad $\approx 1°$.

Correspondingly, the nuclear form factor restricts the momentum transfer

$$|t| \lesssim 0.074 A^{-2/3} (\text{GeV}/c)^2 \approx$$

$$\approx 0.014 \text{ for carbon, } 0.0022 \text{ for lead.} \tag{11}$$

For light nuclei, the component of the momentum transfer parallel to the beam, $q_{||}$, which the nucleus can stand without breaking up, is similarly restricted by the uncertainty principle

$$q_{||} a \lesssim \pi. \tag{12}$$

For heavier nuclei, where absorption is important, a should be replaced by a few times the mean free path for interaction in the nucleus in Eqs (12)–(14). Alternately we can derive (12) by noting that in order for reaction (1) to be appreciably coherent over a spatial region of the order of the nuclear diameter, a, the phase shift (qa) between incident (b) and outgoing (s) waves across the nucleus must not be larger than $\sim \pi$, ($\sin \theta > 0$ for $0 < \theta < \pi$). From equation (4) we see then that the nuclear form factor puts an approximate limit to the mass M_s that can be produced from a given nucleus at a given beam momentum

$$M_s^2 \lesssim M_b^2 + 2 q_{||} p_b \lesssim M_b^2 + 2 \left(\frac{\pi}{a}\right) p_b \approx M_b^2 + 2(0.28 A^{-1/3}) p_b. \tag{13}$$

Thus the M_s that can be produced from a given nucleus goes as $\sqrt{p_b}$ and for a given p_b, as $A^{-1/3}$. For $M_s^2 = 1$ GeV^2, $p_b = 5$ GeV/c, we find $q_{||} = 0.1$ GeV $\approx$ the characteristic momentum transfer for light nuclei.

From equations (7) and (4) we see that the cross-section for reaction (1) contains a beam momentum dependent factor

$$\sigma \sim e^{-B(M_s^2/2p_b)^2}. \tag{14}$$

Thus from this $t_{\min}$ effect alone, the cross-section for $\pi \to A_1$, or $K \to Q$ from light nuclei should increase by roughly a factor 2 from ~ 5 to ~ 15 GeV. Heavy liquid bubble chamber experiments have confirmed this [26, 27].

In addition to this $\exp(Bt_{\min})$ factor in the beam momentum dependence of the coherent cross-section for a particular reaction (1), we expect, on a Regge picture that

$$\sigma = \int dt \frac{d\sigma}{dt} \approx \frac{1}{B} \frac{d\sigma}{dt}\bigg|_{t_{\min}} \sim S^{2\alpha(0)-2} \approx p_b^{2\alpha(0)-2} \tag{15}$$

because the nuclear form factor restricts t (*cf.* Eq. (11)) to values near 0. Here $\alpha(0)$ is the Regge trajectory intercept at $t = 0$. For Pomeron exchange reactions we expect $\alpha(0) \approx 1$ so $\sigma \sim$ constant, for ω exchange $\alpha(0) \approx 0.5$ so we expect $\sigma \sim 1/p_b$ for a particular reaction (1), *i.e.* for a particular band of M_s. Note that the total cross-section for a particular reaction (1), *i.e.* integrated over M_s, should thus increase with p_b (for Pomeron exchange processes) as the $\exp(Bt_{\min})$ factor permits higher and higher masses to be coherently produced while cross-sections for production of lower M_s saturate and remain constant with increasing beam momenta.

Thus we have seen that the dominant coherent production reactions, *i.e.* those which can proceed *via* vacuum exchange, should have cross-sections rising at first according to equation (14) then saturating and remaining roughly constant with p_b for a particular M_s band *and* slowly rising with energy for all M_s and should have momentum transfer distributions dominated by the nuclear form factor (Eq. (7)).

4. Selection rules for coherent production reactions

In order for the amplitudes for $b \to s$ production to sum coherently over the nucleus, the struck nucleon must not have its state changed in such a way that which one it was could be determined in principle by measurements on the residual nucleus or nuclear debris.

Thus the struck nucleon must not, for example, have its charge or strangeness altered. Correspondingly the "particle" exchanged between the nucleus and b in reaction (1) must have $I_{z\,\mathrm{ex}} = S_{\mathrm{ex}} = 0$. (We neglect possible transitions between isobaric analog states which could proceed *via* $I = 1$ exchange [29] and conceivable similar transitions to analog hypernuclear states.) Thus in the transition $b \to s$,

$$\Delta I_z = \Delta S = 0. \tag{16}$$

Because nuclei are not eigenstates of C (charge conjugation) or $G = C \exp(i\pi I_y)$, the exchanged particle can have C either $+$ or $-$ and G either $+$ or $-$; thus in the transition $b \to s$

$$\begin{aligned} C\,\text{flip} &= \text{yes or no} \\ G\,\text{flip} &= \text{yes or no.} \end{aligned} \tag{17}$$

Because the amplitude for an isospin 1 particle to couple to a proton has sign opposite to its amplitude to couple to a neutron we expect the selection rule $I_{\mathrm{ex}} = 0$ or

$$\Delta I = 0. \tag{18}$$

This rule is exact for nuclei with $N = Z$ and approximate otherwise (good roughly to order $(N-Z)/A$ in amplitude, thus to at least this order in cross-section). We assume here that the neutron and proton distributions over the nuclear volume are the same. Violations of this selection rule may provide a means for observing such n, p distribution differences.

For a spin 0 nucleus (*e.g.* ^{4}He, ^{12}C, ^{20}Ne, ^{208}Pb) to recoil coherently in its ground state only natural parity, *i.e.* $J^P_{ex} = 0^+, 1^-, 2^+$, *etc.*, can be exchanged in the t channel *i.e.* $0^+ + 0^+$ can make only $J = l, P = (-1)^l$. This is true not only in the forward direction but at finite angles and is not modified by absorption effects. Nuclei with non-zero spin can exchange unnatural parity *i.e.* $J^P_{ex} = 0^-, 1^+, 2^-$, *etc.*, but only to the extent that the nuclear spin is coupled or, away from the forward direction, using the factor $\boldsymbol{p}_b \times \boldsymbol{q}$ to provide the unnatural parity. Unnatural parity exchange is decreased in addition by a factor roughly (nuclear spin/2A) in amplitude. Where absorption is important, however, A is reduced to an A effective while the nuclear spin presumably comes mainly from outer nucleons where absorption effects are less important. Thus this suppression factor may not be much bigger than typically ~ 10 in amplitude even for heavy nuclei. Nevertheless selection rule (19) is a good approximation (better than 1% except possibly for the deuteron) for the intensity when the additional suppression due to smaller spin couplings is taken into account. Thus we expect

$$\begin{aligned} J^P_{ex} &= 0^+, 1^-, 2^+, \textit{etc}..., \text{ only} \\ \Delta J_{b\,\text{to}\,s} &= \text{any integer} \\ \Delta P_{b\,\text{to}\,s} &= (-1)^{\Delta J}. \end{aligned} \tag{19}$$

The amplitude for reaction (1), expressed in terms of helicity amplitudes can be written [3]

$$f_{\lambda_s \lambda_R; \lambda_b \lambda_T} \sim \left(\sin \frac{\theta}{2}\right)^{|\lambda - \mu|} \tag{20}$$

where the λ's are helicity indices for the incoming and outgoing particles of reaction (1) and $\lambda = \lambda_b - \lambda_T$, $\mu = \lambda_s - \lambda_R$. For coherent reactions the nuclear spin, if not zero, is uncoupled (to a good approximation except possibly for the deuteron), so $\lambda - \mu = \lambda_b - \lambda_s$. Thus if the outgoing states has $\lambda_s \neq \lambda_b$, *e.g.* non-zero helicity for π or K beams, the coherent amplitude must vanish in the forward direction. This leads to the approximate selection rule

$$\lambda_s = \lambda_b. \tag{21}$$

An experimentalist's mnemonic for $\lambda_s = \lambda_b$ (and (19)) is to picture the coherent production reactions as proceeding by "elementary vacuum", *i.e.* $J^P = 0^+$ exchange. Viewed from the s rest system ("RS") we have a head-on collision of the beam particle and a 0^+ particle. Their relative orbital angular momentum, l, is perpendicular to their momenta so $m = J_z = 0$ for π or K beams, $= \pm 1/2$ for p or $\bar{p}$ beams, $= \pm 1$ for photon beams. For π or K beams only $J = l$, $P = -(-1)^l$ is then allowed for s *i.e.* s must have unnatural parity (0^-, 1^+, 2^- *etc.*). For nucleon (or antinucleon) beams any J^P_s is allowed (*e.g.* $^3/_2{}^+$ *via* $l = 2$, $^3/_2{}^-$ *via* $l = 1$), but $\lambda_s = \pm {}^1/_2$ *i.e.* the outgoing state is aligned with the same J_z as the beam.

TABLE I

$\pi \to 3\pi, 5\pi$ (vacuum exchange)

Beam momentum (GeV/c) target	Reference (*et al.* always)	No coherent events	Fraction of d recoils not seen	Cross-section (μb/nucleus) Observed	Corrected	A_1 region (d*out, ϱ in)	Slope B (GeV/c)$^{-2}$ of t distribution	Slope B' (GeV/c)$^{-2}$ of t' distribution
3.7 $\pi^- d$	Abolins 1965 [32]	158	?		~420	~100		
3.85 π^- emulsion	Shahbazian 1967 [33]	1	—		500±500			
4.2 $\pi^+ d$	Eisenstein 1970 [34] and Gordon	696	<0.10	275±60		~68	~20.5	
4.5 $\pi^+ d$	Forino 1965 [35]	181		260±70				
5.0 $\pi^- d$	Vanderhaghen 1969 [36]	746	0.20±0.5	264±10				
$\pi^+ d$	Vanderhaghen 1969 [36]	614		267±11	324±25	147±21	21.0±0.8	36.0±1.5
5.4 $\pi^+ d$	Deery 1970 [37]	793						
6.0 $\pi^+ d$	Vegni 1965 [38]	251			370±50+		32.7±6.5	38.1±5.2
6.0 π^- — $C_{22}F_3Br$	Allard 1965 [26] Bellini 1963, 1965 [27]	~70	HLBC	26±7 mb/$C_{22}F_3Br$ for $t < 0.08$				75±25
7.0 $\pi^+ d$	Firebaugh 1970 [140]	1734	20±1	450				
7.5 π^- emulsion	Mięsowicz 1971 [66]			1.16±05 mb/nucl.				
8.0 $\pi^+ d$	Cnops 1968 [41]	792	3 prong events included		342±40+	150±20 8–1.2 GeV/c	39.5±2.5 A_1 region	
	Cnops 1969 [41]							
11.6 $\pi^- d$	Fung 1971 [42]	737	4 pr only					
11.7 $\pi^+ d$	Kemp 1970 [43]	1808	4 pr	320±100+	440±40	150±30	29±3	33±3
	Barrier 1971 [44]	305	3 pr					
13 $\pi^+ d$	Paler 1971 [45]	1246	3+4 pr					
		101	5+6 pr					
15.1 π^- — Be, C Si, Al, Ti, Ag, Ta, Pb, CERN MSC	Bemporad 1970 [46]	22679	MS	See Fig. 7				

TABLE I (continued)

Beam momentum (GeV/c) target	Reference (*et al.* always)	No. coherent events	Fraction of d recoils not seen	Cross-section (μb/nucleus) Observed	Corrected	A_1 region (d^* out, ϱ in)	Slope B $(\mathrm{GeV}/c)^{-2}$ of t distrib.	Slope B' $(\mathrm{GeV}/c)^{-2}$ of t' distrib.
15, 16 π^- — C_2F_5Cl	Allard 1966 [26]	1135 $\pi^+2\pi^-$	HLBC		4.0 ± 0.6 mb/F	1.58 ± 0.02 mb/F	78 ± 17	
	Daugeras 1968 [47]	246 $\pi^-2\pi^0$	HLBC			0.96 to 1.2 GeV	67 ± 23	
	Huson 1968 [48]	37 — $2\pi^+3\pi^-$	HLBC		0.1 ± 0.03 mb/F	< 3 μb/F	$54 \pm \begin{smallmatrix}90\\45^*\end{smallmatrix}$	
15 π^-Pb	Veillet 1968 [49]	$50\pi^+2\pi^-$	Pb		16 ± 7 mb/Pb			
	Huson 1966 [50]	$3\pi^-\pi^0$			$\lesssim$1 mb/Pb			
17 $\pi^-C_4F_3Br$	Huson and Fretter 1964 [51]	$41\pi^+2\pi^-$ $14\pi^-2\pi^0$	HLBC	22 ± 6 mb/C_4F_3Br	5mb/C or F 3 mb/C or F	for t < 0.08		
18 $\pi^-C_{22}F_3Br$	Allard 1965 [26] Bellini 1963, 1965 [39]		HLBC	55 ± 15 mb/$C_{22}F_3Br$		for t < 0.08		
16 π^- emulsion	Cafario 1964 [52]	$\pi^+2\pi^-$	emulsion	4.11 ± 0.54 mb/nucl.				
	See Anzon 1970 [53] for USSR references. See also Mięsowicz 1971 [66]	$2\pi^+3\pi^-$		0.31 ± 0.03 $A^{2/3}$ mb/nucl. 0.06 ± 0.04 mb/nucl.				
45 π^- emulsion	Anzon 1970 [53]	117 ± 5 $\pi^+2\pi^-$	emulsion	8.95 ± 0.9 mb/nucl. 0.74 ± 0.08 $A^{2/3}$ mb/nucl.				
	Mięsowicz 1971 [66]	11.4 ± 4.6 $2\pi^+3\pi^-$	emulsion	0.90 ± 0.4 mb/nucl.				
60 π^- emulsion	Mięsowicz 1971 [66]	197 ± 16 $\pi^+2\pi^-$	emulsion	13.2 + 0.8 mb/nucl. 1.10 ± 0.07 $A^{2/3}$ mb/nucl.				
		23.7 ± 8.1 $2\pi^+3\pi^-$	emulsion	1.6 ± 0.57 mb/nucl. 0.132 ± 0.045 $A^{2/3}$ mb/nucl.				
200 $\pi^\pm$ emulsion	Czachowska 1967 [59]	~7 $\pi^+\pi^+\pi^-$	emulsion	~2.0 $A^{2/3}$ mb/nucl.				
	Rybicki 1969 [74]	$2\pi^\pm2\pi^+2\pi^-$	emulsion	~0.56 $A^{2/3}$ mb/nucl.				

+ Quoted by Bellini (1969) [8].

* Not corrected for experimental resolution.

TABLE II

$K \to K\pi\pi$ (vacuum exchange)

Beam momentum (GeV/c), target	Reference (*et al.* always)	No coherent events $K\pi\pi$	Channel	Fraction of d recoils not seen	Fraction of events with K–π ambig.	Cross-section (μb/nucl.)		Slope B (GeV/c)$^{-2}$
						observed	corrected	
2.24 K^-d	Rhode 1969 [56]	11	$K^-\pi^+\pi^-$	0	small	40 ± 20	40 ± 20	
2.3 K^+d	Butterworth 1965 [57]	81	$K^+\pi^+\pi^-$	0	small	110 ± 16	110 ± 16	
3.0 K^+d	Buchner 1969 [58]	266	$K^+\pi^+\pi^-$				210 ± 22	
3.0 K^-d	Hoogland 1969 [59]	553	$K^-\pi^+\pi^-$	0.02			102 ± 14	28.4 ± 1.1
		206	$K^0\pi^-\pi^0$				115 ± 20	27.1 ± 3.5
3.8 K^+d	Eisenstein 1970	900	$K^+\pi^+\pi^-$	0.1	~ 0.09			~ 17.5
	+ Robinson [60]	397	$K^0\pi^+\pi^0$					
5.5 $K\ d$	Werner 1969 [61]	719	$K^-\pi^+\pi^-$	0.17	~ 0.26	194 ± 30	228 ± 35	~ 25
5.5 K^-Ne	Cnops 1969 [62]	130	$K^-\pi^+\pi^-$	Neon	~ 0.7		1680 ± 500	~ 90
10.0 K^+ Propane-freon	Haguenauer 1970 [63]	810	$K^+\pi^+\pi^-$	HLBC	~ 0.85		2200 ± 370	94 ± 11
10.0 K^-	Daugeras 1971 [31]	455	$K^-\pi^+\pi^-$	HLBC	~ 0.85		2930 ± 330	~ 100
Propane-freon	Cnops 1969 [62]	29	$K^0\pi^-\pi^0$		0		3160 ± 980	
12.0 K^+d	Firestone 1971 [65]	2081	$K^+\pi^+\pi^-$	Meas			331 ± 8	~ 25
		3 pr		3 pr				
		3525						
		4 pr						
12.7 K^-Ne	Daugeras 1971 [31]	958	$K^-\pi^+\pi^-$	Neon	~ 0.9		3720 ± 260	~ 100
	Cnops 1969 [62]	101	$K^0\pi^-\pi^0$		0		2350 ± 425	
		56	$K^-\pi^0\pi^0$		0		770 ± 240	
12.7 K^-d	Antich 1970 [64]	415	$K^-\pi^+\pi^-$	0.34	~ 0.36	186 ± 70	285 ± 70	31 ± 3
		115	$K^0\pi^-\pi^0$	0.34	0	205 ± 50	297 ± 80	

More precisely, one can note [30] that for an unnatural parity 0^- beam (*e.g.* π, K) producing a final state s of unnatural parity (*e.g.* A_1, Q), the forward amplitude need not vanish for $\lambda_s = 0$ while it must vanish for $|\lambda_s| \geqslant 1$. For 0^- beam producing a state of natural parity (*e.g.* $\pi \to \varrho$, $K \to K^*(890)$ *via* natural parity exchange $\lambda_s = 0$ is forbidden (to make *e.g.* $J_s^P = 1^-$ from 0^- plus (natural J_{ex}^P) requires relative orbital angular momentum $l = J_{ex}$ or $J_{ex} \pm 1$. Parity conservation (requires $l + J_{ex}$ = even, so $l = J_{ex}$. Since $l_z = 0$ to make a vector meson with $J_z = 0$ would require $J_{zex} = 0$ which is forbidden: the Clebsch-Gordan coefficient

$$\langle l = J_{ex}, J_{ex}, 0, 0, |J_s = 0, J_{zex} = 0\rangle \text{ is zero for } l + J_{ex} + J_s = \text{odd}).$$

In general [30] $J_z = 0$ states are not populated when a natural (unnatural) parity state is produced by a 0^- beam *via* natural (unnatural) parity exchange.

Thus to return to the case of a $0^- \to 1^-$ transition, only unnatural parity exchange can contribute to a non-zero forward amplitude while natural parity exchange populates only $\lambda_s = \pm 1$ which by (20) must vanish in the forward direction. Thus we expect 1^- (and other natural parity states) production to be heavily suppressed relative to 1^+ (and other unnatural parity states).

We conclude that of all the 30 odd mesons listed in the wallet card only a few can contribute to the dominant coherent production reactions. Exchange of isovector mesons π, ϱ, δ, A_1, A_2, B, *etc.* is forbidden (approximately) by (18); exchange of isoscalar but unnatural parity mesons η, η', D, E, *etc.* is forbidden by (19). Note that π exchange, which dominates many free nucleon reactions is doubly forbidden — it violates $\Delta I = 0$ (18) and is unnatural parity exchange (*viz.* (19)). Of clearly established mesons (or exchanges) only the isoscalar natural parity mesons P, P', f^0 (and ε^0) (with $G = +$, $C = +$) and ω^0, φ^0 (with $G = -$, $C = -$) can be expected to contribute importantly. For K and nucleon beams there is no difference between $G = +$ and $-$ exchange (although C exchange is

TABLE III

Rare coherent K channels

Beam momentum and target	Reference (*et al.* always)	Channel	Cross-section (μb/nucl.)
10 K^+ propane-freon	Haguenauer 1970 [63]	$K^+\pi^+\pi^-\pi^0$	280 ± 130
12.7 K^-d	Antich 1970 [64]	$K^-\pi^+\pi^-\pi^0$	21 ± 8
		$K^0\pi^-\pi^+\pi^-$	13^{+10}_{-6}
		$\bar{\Lambda}p$	2^{+2}_{-1}
		$K^-p\bar{p}$	$\leqslant 1$
12.7 K^- neon	Daugeras 1971 [31]	$K^-\pi^+\pi^-\pi^0$ $(K^-\omega)$*	238 ± 60
		$K^0\pi^-\pi^-\pi^-$ $(L \to K3\pi)$	90 ± 40

* Mass $K\omega < 1.56$ GeV corresponding to a branching ratio for the Q region of $\dfrac{K^-\omega^0}{K^-\pi^+\pi^+} = 7.5 \pm 1.8\%$

TABLE IV

$K \rightarrow K\pi$ (ω exchange)

Density matrix elements are given for Jackson system, K^*RS
Pure ω exchange predicts $\varrho_{11} = |\varrho_{1-1}| = 0.5$, $\varrho_{00} = \text{Re}\,\varrho_{10} = 0$

Beam momentum and target	Reference (*et al.* always)	No events $K_1^0\pi^\pm$	No events $K^*(890)^\pm$	σ (μb/nucl.)	$\sigma_{K^*(890)}$ (μb/nucl.)	ϱ_{00}	ϱ_{1-1}	Re ϱ_{10}
2.3 K^+d	Butterworth 1965 [57]	33	31	150 ± 35	~141			
3.0 K^+d	Buchner 1969 [58]	74	40	228 ± 25	~124	0.26 ± 0.11	0.27 ± 0.08	$+0.04\pm0.05$
3.0 K^-d	Hoogland 1969 [59]	154	150	112 ± 20	~110	0.11 ± 0.07	0.27 ± 0.06	-0.05 ± 0.06
4.5 K^-d	Eisner 1968 [67]	76	53	33 ± 5	~23	0.12 ± 0.1	0.38 ± 0.1	$+0.04\pm0.04$
12.0 K^+d	Firestone 1970 [65]	~120		20 ± 5	$\sim20\pm5$		~0.43	
12.7 K^-d	Antich 1970 [64]	46	12	15 ± 6	$\sim13\pm6$			
12.7 K^-Ne	Daugeras 1971 [31]	~40 $K^0\pi^-+K^-\pi^0$			180 ± 70			

required to regenerate K_1^0 from K_2^0). For π beams $\pi \to \pi, 3\pi, 5\pi$, *etc.*, only is allowed ($\pi \to 2\pi, 4\pi$ *etc.* forbidden) for $G = +$ exchange and only the reverse for $G = -$ exchange. For brevity in what follows I will refer to the first ($G = +$) group as "vacuum", the second ($G = -$) as "ω^0" exchange. Note that as far as selection rules are concerned, Coulomb production (*i.e.* γ exchange) is like (predominantly) ω^0 exchange (with order $(N-Z)/A$ contribution of ϱ^0 exchange).

5. *Available data on coherent production reactions*

Data available as of Spring 1971 ("pre Amsterdam") on coherent production reactions in π, K and nucleon (antinucleon) beams is summarized in Tables I–V: dominant ("vacuum exchange") reactions $\pi \to 3\pi$, $\pi \to 5\pi$ (Table I); $K \to K\pi\pi$ (Table II); rare K coherent reactions (Table III); "ω exchange" reactions (Table IV); and nucleon (antinucleon) induced reactions (Table V).

TABLE V

Coherent production $p, \bar{p}$

Beam momentum (GeV/c), target	Reference (*et al.* always)	No coherent events	Channel	Cross-section d visible	(μb/nucl.) corrected
1.8 pd	Brunt 1968 [68]	112*	$p\pi^+\pi^-$	185±18	
		2	$p\pi^+\pi^-\pi^0$	3±2	
2.1 pd	Brunt 1968 [68]	97*	$p\pi^+\pi^-$	170±18.	
		14	$p\pi^+\pi^-\pi^0$	25±5	
5.55 $\bar{p}d$	Evrard 1969,				
	Braun 1970 [69]	359	$p\pi^+\pi^-$	113±38	220±20
7.0 $\bar{p}d$	Antich 1970b				
	[64]	310	$p\pi^+\pi^-$	260±25	355±40
		172	$p\pi^+\pi^-\pi^0$	180±22	250±25
		4	ΛK^-	3±2	40
		2	$\Lambda K^-\pi^0$	2±2	
28 pNe	Huson 1968 [70]	35±6**	$p\pi^+\pi^-$		470±100
		57±8***	$p\pi^+\pi^-$		750±120
28 n C	O'Brien 1971	Many thousands	$p\pi^-$		
Cu	[71]				
Pb					

* Not counting those with fast d and invisible proton.

** Mp $\pi\pi < 1.6$.

*** Mp $\pi\pi < 2.6$.

6. *Techniques*

Most of the experiments cited used deuterium bubble chambers ("DBC"), propane-freon or hydrogen-neon bubble chambers ("HLBC") or nuclear emulsions. The shape of things to come, however, is suggested by entries of two counter-spark chamber experiments. There is (unfortunately) no published coherent work using helium (or xenon) BC's, nor helium (or neon) discharge chambers.

Emulsion experiments are discussed in Professor Mięsowicz lectures [66] so will not be discussed here. Emulsions have the advantage of good spatial resolution (protons of $\gtrsim 0.1$ MeV and light nuclear recoils of $\gtrsim 1$ MeV are observable, which aids in the separation of coherent from nuclear breakup reactions). Statistics are normally very limited, however, and π^0's are not detected directly so that normally little detail on the characteristics of coherent reactions is accessible to emulsion experiments [13].

DBC experiments nowadays have up to some 10–20 events per microbarn (μb) of cross-section, are unbiased compared with other techniques and about as precise as any other technique. They can detect the deuterium recoil down to ~ 130 MeV/c (1 mm range) and for events with no π^0's produced at least, can work with the events with unseen deuteron ("3, 5, *etc.* prong events"). Some experimenters do not measure the 3 prong events, however, which typically forces them to make $\sim 30\%$ corrections in extracting cross-sections. The major limitation of DBC's is that π^0's are not detected directly and at most one π^0 can be reconstructed kinematically (and this not very clearly at high energies). There are proposals to surround a DBC with transparent walls (perhaps of scintillators to participate in triggering) and an outer region of H_2-Neon for γ (thus π^0, η^0, ... *etc.*) detection to remove this limitation but as yet no such experiment has been published.

HLBC's can measure final states with one or more π^0's (although beyond 2 π^0's sorting out the γ's becomes quite difficult at high energies). The π^0's are reconstructed about as accurately as charged tracks in the same chamber. Precision on charged tracks is typically ~ 5 times worse in HLBC's than in DBC's, however. The nuclear recoil is not detected directly but since π^0's are observed it is normally the only missing "neutral" and can be reconstructed accurately enough to separate coherent from most incoherent events. Aside from relatively poor precision, the major limitation of HLBC's is that the choice of target liquids is limited so far to (He), C, Ne (and Xe) for "pure" liquids (*i.e.* containing only this nucleus plus possibly hydrogen) and to mixtures of C, F, Cl, Br, *etc.* for freons.

Counter-spark chamber experiments can vary A freely and can accumulate statistics at least an order of magnitude faster than BC's. They can be triggered on coherent candidates, *e.g.* by vetoing events with large momentum transfer, γ's at wide angles, counting and identifying outgoing tracks, *etc.* So far no counter study of coherent final states including π^0's has been published, however, and those involving only charged tracks have had relatively large corrections for apparatus asymmetries and biases. It is clear, however, that much future information on coherent reactions will come from electronics experiments.

7. *Dominant ("vacuum exchange") reactions*

The characteristics of the dominant coherent production reactions $\pi \to 3\pi$, 5π (Table I), $K \to K\pi\pi$ (Table II) and $n \to n\pi$, or $n \to n\pi\pi$ (Table V) are epitomized in Figs 2–18. Fig. 2 shows typical distributions of t, the momentum transfer from target to recoil nucleus (or $t' = t - t_{min}$). As expected (see theoretical t' distributions in Fig. 1, calculated by Fournier [7] in a manner similar to that described in Professor Goldhaber's lectures), there

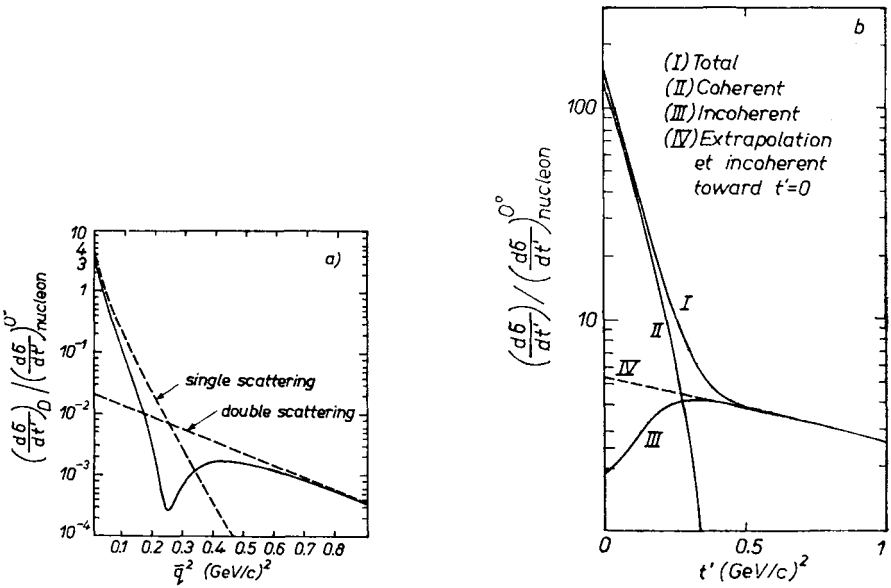

Fig. 1a. Differential cross-section for coherent production from deuterium (divided by corresponding production differential cross-section from hydrogen). Calculation of Fournier [7] for $\sigma_b = 25$ mb, $\sigma_s = 40$ mb, $\alpha_b = \alpha_s = +0.2$, $M_b = 0.493$ GeV, $M_s = 1.3$ GeV, free nucleon scattering slopes $\lambda_b = \lambda_s = 8$ (GeV/c)$^{-2}$, $\lambda_{bs} = 10$ (GeV/c)$^{-2}$, $p_b = 12.7$ GeV/c. Note that the double scattering (*i.e.* production from one nucleon preceded or followed by elastic scattering from the other) term reduces the forward ratio from 4 to about 3.3, produces a dip (at $t \approx -0.25$) where the single and double scattering amplitudes are equal in magnitude, and dominates beyond; **b.** Differential cross-section for coherent and incoherent production (divided by the forward hydrogen differential production cross-section) from Neon for $q_{||} = 56$ MeV/c, $\sigma_b = \sigma_s = 20.9$ mb, $\alpha_b = \alpha_s = 0$, $\lambda_b = \lambda_s = 7.3$ (GeV/c)$^{-2}$. From Fournier [7]. The difference between the "2 exponential fit" estimate of the incoherent background under the coherent peak (curve *IV*) and the Trefil model estimate (curve *III*) is about 5 per cent of the coherent cross-section for $t' < 0.04$ (GeV/c)^2

is a steep slope at small t characteristic of diffraction from an object of the size of the nucleus as a whole and at large t a slope characteristic of free nucleon interactions (coming from incoherent reactions on quasi-free nucleons in the nucleus). In between there may be successive changes of slope or diffraction maxima and minima coming from two and multistep processes in the nucleus (*cf.*, the hint of such structure in the CERN-ETA-ICL-Milan ("CEIM") data for $\pi \to 3\pi$ in Fig. 2d).

Typical distributions of the mass of the outgoing state (s in Eq. (1)), are shown in Figs 3 ($\pi \to 3\pi$), 9($\pi \to 5\pi$), 10 ($K \to K\pi\pi$), 17 ($n \to p\pi$, $p \to p\pi\pi$). Note that there is a first peak in each case starting roughly at threshold for the least massive quasi-2-body state out of which it can be made (*e.g.* $\pi\varrho$ for 3π, ϱA for 5π, $K^*(890)$ π or $K\varrho$ for $K\pi\pi$, $\Delta\pi$ for $p\pi\pi$, *etc.*). In most cases at high enough beam momenta there is a second peak (*e.g.* πf^0 for 3π, $K^*(1400)\pi$ for $K\pi\pi$, *etc.*) corresponding to the next leastmassive quasi-2-body possible constituents, *etc.* Each peak is typically at its maximum a pion mass or so above the threshold and is typically 2 or $3m_\pi$ broad. There are a few cases where narrower peaks are observed superposed on the broad "normal" bump (*e.g.* Fig. 3l showing an ~ 120 MeV

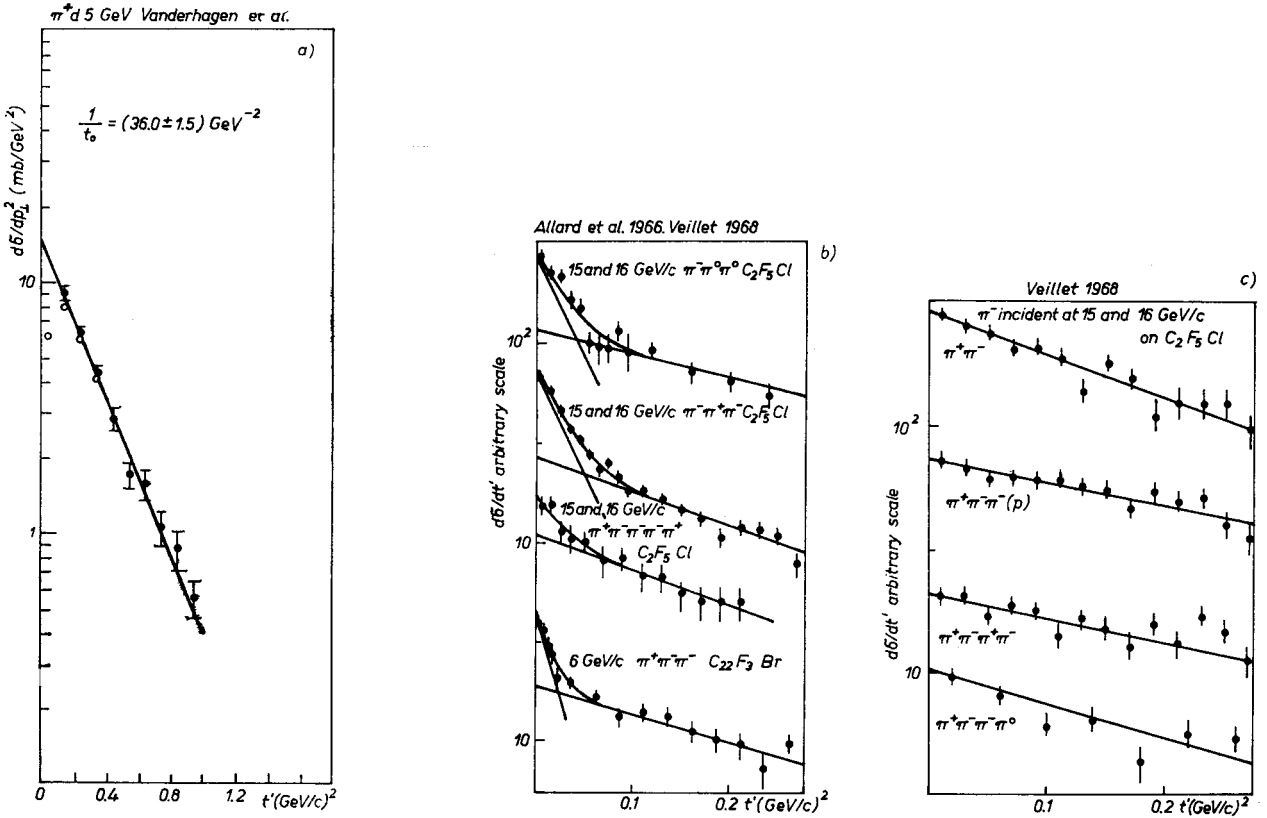

Fig. 2. Typical distributions of momentum transfer t' from target to recoil (minus its minimum kinematically allowed value; see Eqs (4) and (6)). Figures **2a, b, c** are courtesy Bellini [8]; **a.** $\pi^+d \to \pi^+\pi^+\pi^-d$, 5.1 GeV, Vanderhaghen *et al.* [36]. Note absence of incoherent background because deuteron recoil is directly detected; **b.** π^--heavy liquid bubble chamber $\to (3\pi)^-$, $(5\pi)^-$ at 6, 15 and 16 GeV (Allard *et al.* [26], Veillet [12]). Note sharp forward peak due to coherent production, superposed on shallower background due mainly to incoherent processes (the recoil nucleus is not directly detected); **c.** π^-—HLBC $\to (2\pi)^0$, $(4\pi)^0$ which cannot be coherent *via* vacuum exchange with the nucleus. Also $(3\pi)^-$ with visible protons (s) proving nuclear breakup. Note that in contrast to Fig. **2b** from the same experiment, none of these channels shows a coherent peak

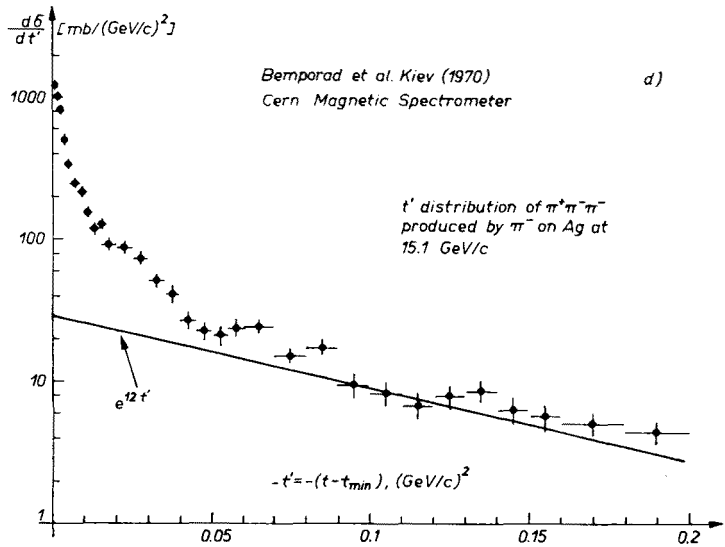

Fig. 2d. $\pi^- - Ag \rightarrow \pi^+\pi^-\pi^-$ Ag at 15.1 GeV (Bemporad *et al.* [46]). The statistics and resolution in this CERN magnetic spark chamber experiment are sufficient to observe several diffraction-like minima. Incoherent background is present at large t' as in HLBC's

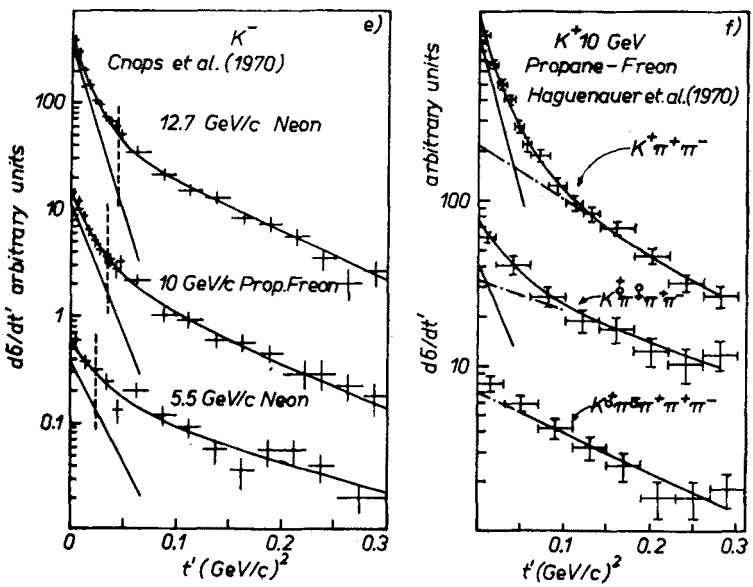

Fig. 2e. K^-(HLBC)$\rightarrow K^-\pi^+\pi^-$ at 12.7, 10, 5.5 GeV (Cnops *et al.* [62]) showing coherent and incoherent production; f. K^+(HLBC)$\rightarrow K^+\pi^+\pi^-$ at 10 GeV (Haguenauer *et al.* [63]) showing clear coherent peak, $\rightarrow K^+\pi^0\pi^+\pi^-$ showing indication of coherence and $\rightarrow K^+\pi^0\pi^0\pi^+\pi^+\pi^-$ showing no evidence for coherence. See also Fig. 2m

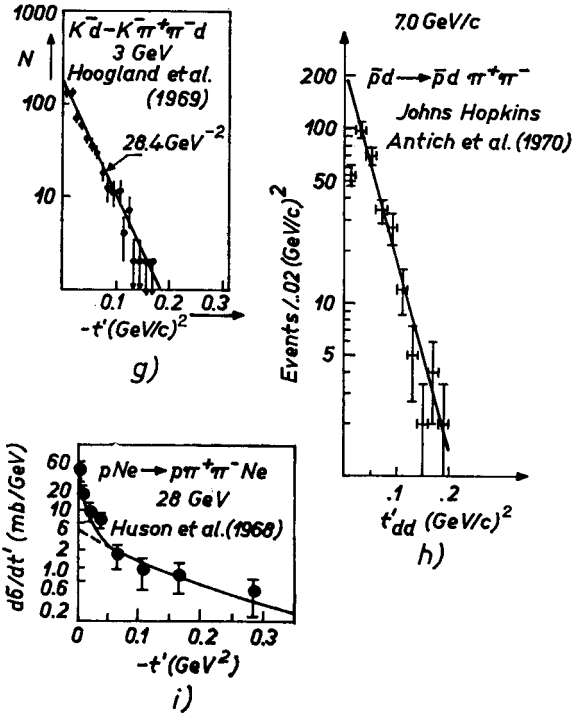

Fig. 2g. $K^-d \to K^-\pi^+\pi^-d$ at 4 GeV (Hoogland *et al.* [59]); **h.** $\bar{p}d \to \bar{p}\pi^+\pi^-d$ at 7 GeV (Antich *et al.* [64]); **i.** $p\mathrm{Ne} \to p\pi^+\pi^-\mathrm{Ne}$ at 28 GeV (Huson *et al.* [70])

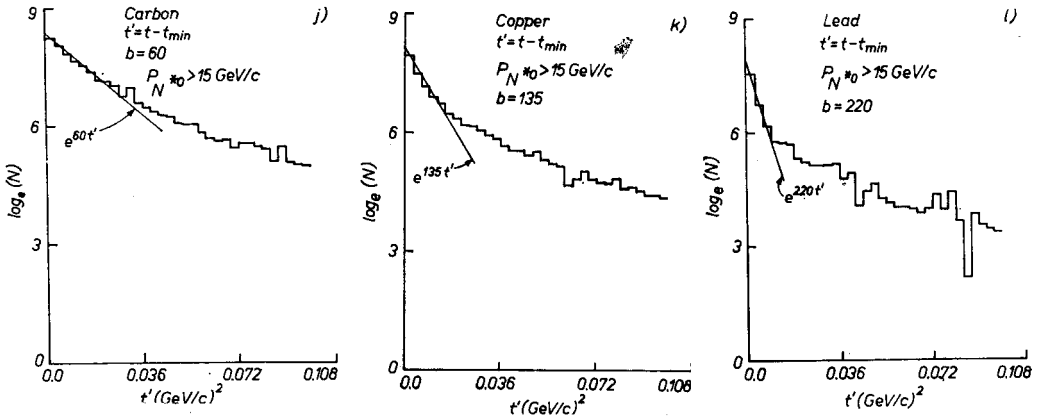

Fig. 2j–l. $nA \to p\pi^-A$ for A = C, Cu, Pb at ~ 27 GeV (O'Brien *et al.* [71])

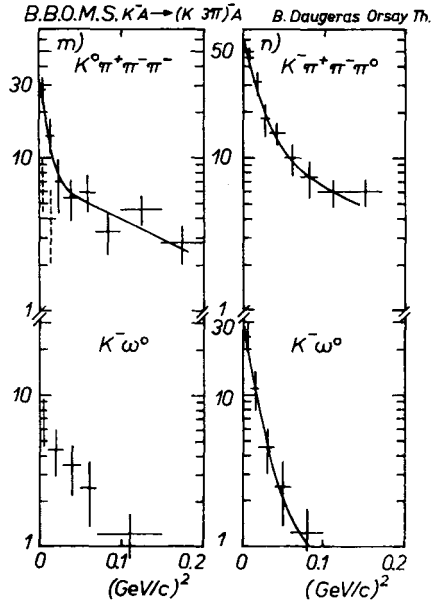

Fig. 2m, n. $K^-A \to (K3\pi)^- A$ for A = freon and neon, 10 and 12.7 GeV (Daugeras [31]). The curves are two exponential fits. In Fig. 2m the dotted points are from the L mass region. Note coherence in $K\omega^0$ subsamples

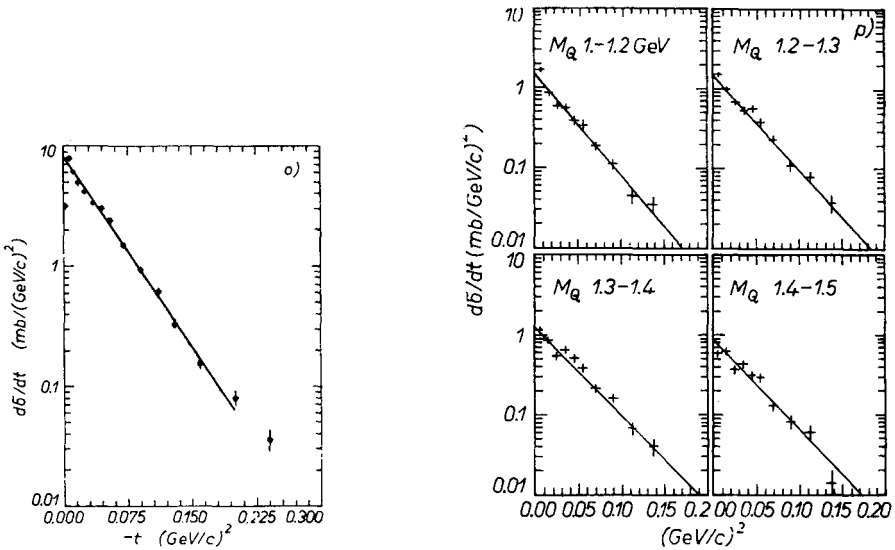

Fig. 2o, p. $K^+d \to K^+\pi^+\pi^-d$ at 12 GeV, LRL [65], Fig. 2p shows lack of large variation of slope with mass of $K\pi\pi$ system from 1 to 1.5 GeV

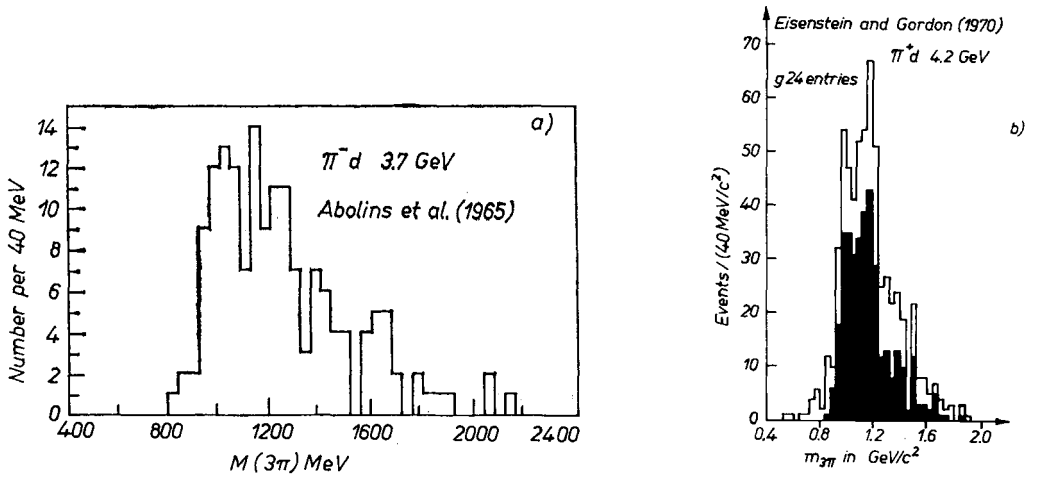

Fig. 3. Mass of $\pi^{\pm}\pi^+\pi^-$ system coherently produced. **a.** $\pi^- d$ 3.7 GeV (Abolins *et al.* [32]), no cuts; **b.** $\pi^+ d$ 4.2 GeV (Eisenstein and Gordon [34]). Outer histogram no cuts, shaded histogram ϱ^0 in, and smaller momentum transfer to this dipion

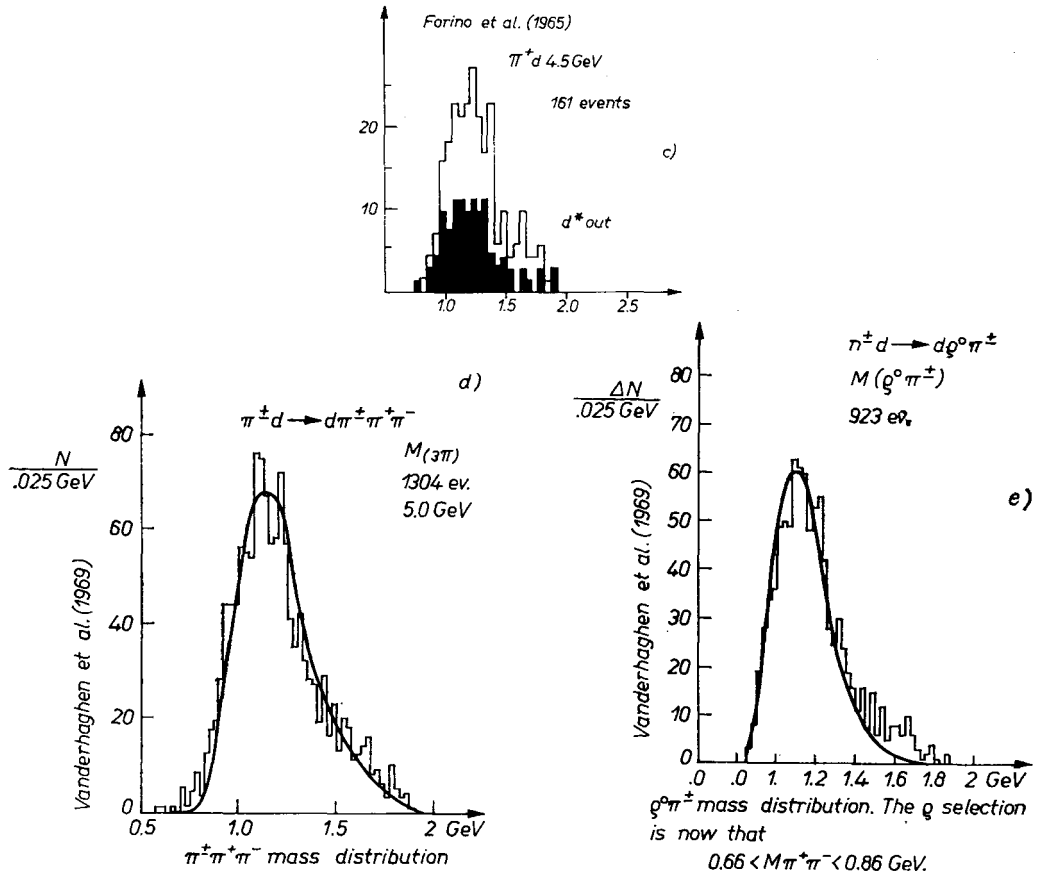

Fig. 3c. $\pi^+ d$ 4.5 GeV (Forino *et al.* [35]). Shaded histogram for d^* out ($Md\pi^+ > 2.4$ GeV); **d.** $\pi^{\pm} d$ 5.0 GeV (Vanderhaghen *et al.* [36]) no cuts; **e.** ditto ϱ^0 in

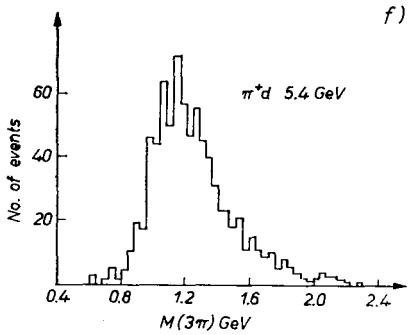

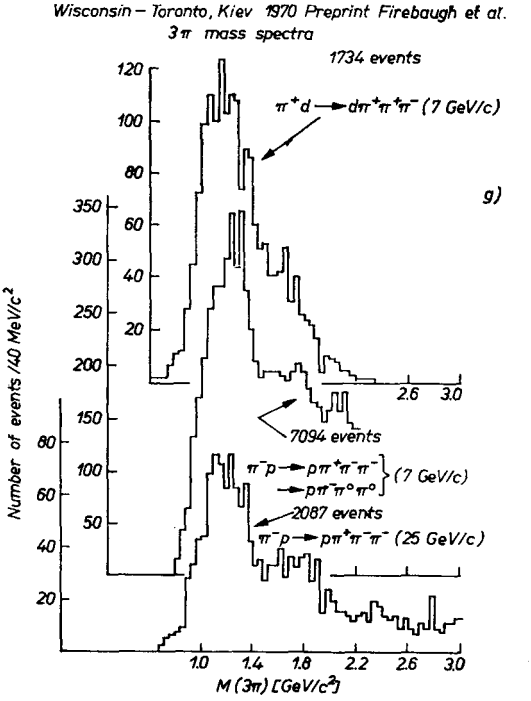

Fig. 3f. π^+d 5.4 GeV (Deery *et al.* [37]); g. π^+d 7 GeV (Firebaugh *et al.* [40]) compared with π^-p 7 GeV and 25 GeV

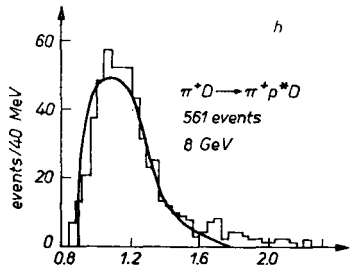

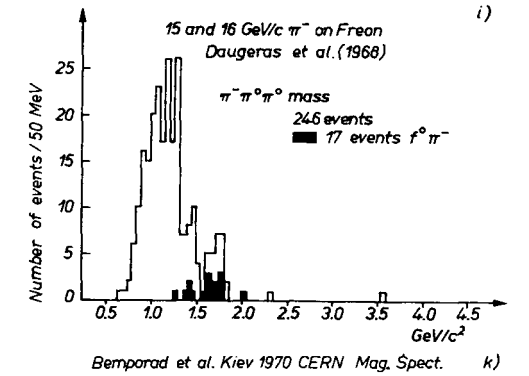

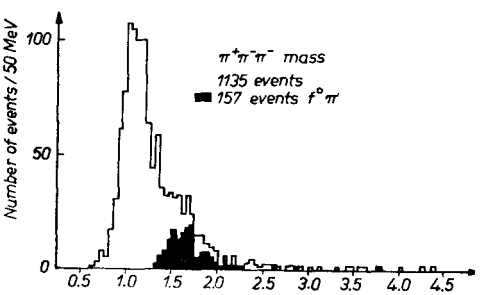

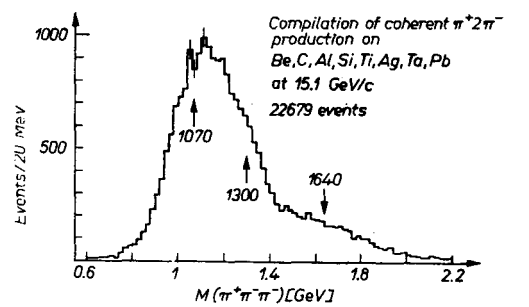

Fig. 3h. π^+d 8 GeV (Cnops *et al.* [41]). ϱ^0 in; i. π^- Freon 15, 16 GeV (Daugeras *et al.* [47]). $\pi^-2\pi^0$ mass, shaded events have $m2\pi^0$ in f^0 region; j. Ditto for $\pi^+2\pi^-$ mass, shaded events have $M\,\pi^+\pi^-$ in f^0 region. Shaded events peak in A_3 region, unshaded in A_1 region, for both $\pi^-2\pi^0$ and $\pi^+2\pi^-$; k. Compilation of coherent $\pi^+2\pi^-$ production on Be, C, Al, Si, Ti, Ag, Ta, Pb at 15.1 GeV/c (from Bemporad *et al.* [46]).

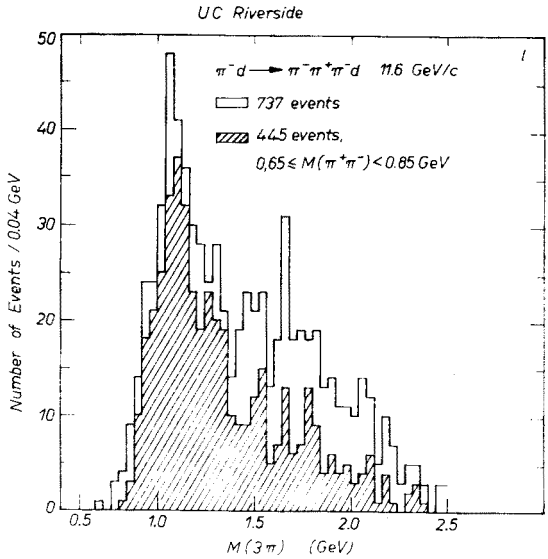

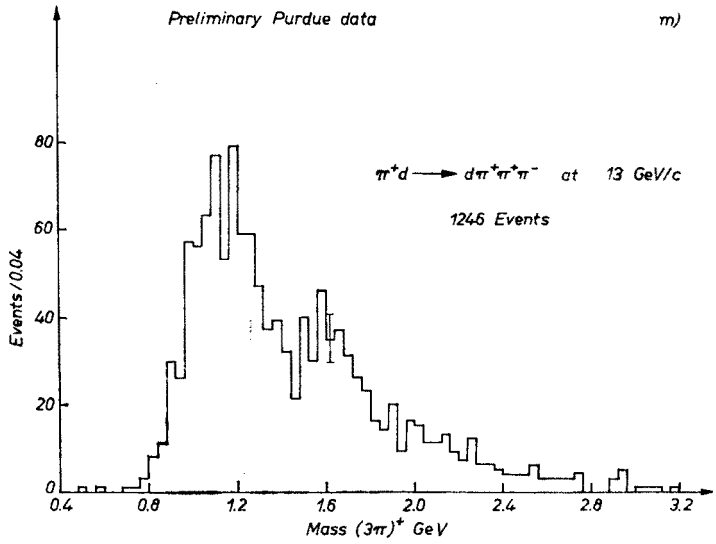

Fig. 31. $\pi^- d$ 11.6 GeV UC Riverside [42]. Note relatively narrow A_1 peak ($\Gamma \sim 120$ MeV) in contrast to most other experiments; **m**. $\pi^+ d$ 13 GeV (Purdue [45]). Note A_3 signal near 1.6 GeV

wide A_1 observed in $\pi^- d$ at 11.6 GeV by a UC Riverside group and Fig. 10f showing a 54 MeV wide Q observed in $K^+ d$ at 3.8 GeV by an Illinois group).

Typical distributions of the 2 out of 3 body masses are shown in Figs 4 ($\pi\pi$ out of 3π), 11 ($\pi\pi$ and $K\pi$ out of $K\pi\pi$), 17 ($p\pi/p\pi\pi$). The dominance of ϱ in the A_1 region, of $K^*(890)$ in the Q region and $\Delta(1238)$ in the "$N^*(1470)$" region is evident. The presence

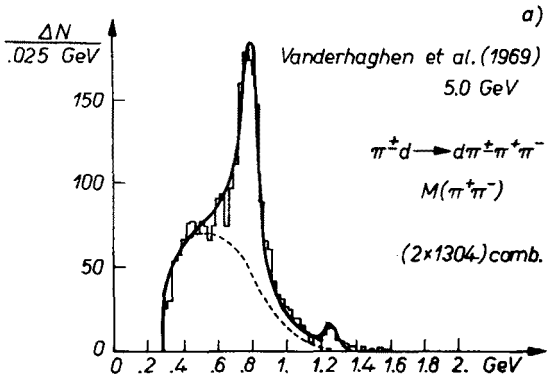

Fig. 4. Representative $\pi^+\pi^-$ distributions from $\pi^\pm \rightarrow (3\pi)^\pm$. **a.** $\pi^+ s$ 5.0 (Vanderhaghen *et al.* [36]) showing ϱ^0 and f^0 peaks over background (dotted curve) of reflections of other resonances. Solid curve shows fit with simple Breit-Wigners

of f^0 in the A_3 and $K^*(1400)$ in the L regions is also clear. There is some evidence for ϱ^0 also in the A_3 and $K^*(890)$ also in the L regions. That one must be very careful in determining $L \rightarrow K^*(890)\pi$ to $L \rightarrow K^*(1400)\pi$ is shown in Figs 11 **j–m** (preliminary data on $K^+ d \rightarrow K^+\pi^+\pi^- d$ at 12 GeV from LRL [65]). The L and $K^*(1400)$ signals are both associated with the d^* band (mass $\pi^+ d$ peaking near the sum of $\pi^+ p$ in Δ_{33} and a nucleon [25]), while the $K^*(890)$ signal is not particularly. The $K^*(1400)$ signal is associated with the L region while again the $K^*(890)$ is not particularly. When the $K^+\pi^-$ mass spectra for $K\pi\pi$ mass regions above and below the L are subtracted from the $K^-\pi^-$ mass distribution for the L region, a strong $K^*(1400)$ signal remains, clearly associated with the L while the $K^*(890)$ signal is strongly reduced. The true $L \rightarrow K^*(890)\pi$ branching ratio is thus probably about 20% and may be much smaller.

Figs 5, 6, 12, 18 give evidence, from angular distributions and Dalitz plot densities, that the spin and parity of the 3-body system corresponds to that obtained by combining its least massive quasi-2-body constituents in relative S wave (*e.g.* $\pi(0^-)+\varrho(1^-)$ in S wave $\rightarrow A_1(1^+)$). Labelling $x = \varrho$, $K^*(890)$ *etc.* as the case may be, we have $\hat{x} \cdot$ beâm in 3-body rest system typically roughly flat as expected for S wave; (beam) · (decay π) in x rest system $\sim \cos^2$ for π or K beams, $1+3\cos^2$ for nucleon beams as expected for alignment in $J_z = 0$ ($\pm 1/2$ for nucleon) states as discussed in the selection rules section above. The corresponding azimuths are roughly flat as expected also. All experiments see asymmetries in these distributions indicating, *e.g.* in the case of $A_1 \rightarrow 3\pi$, interference of the dominant $\pi\varrho$ in S wave with a small amount of $\pi\varrho$ in P wave (corresponding to an admixture of

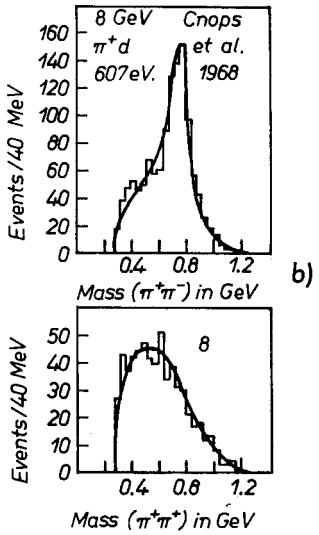

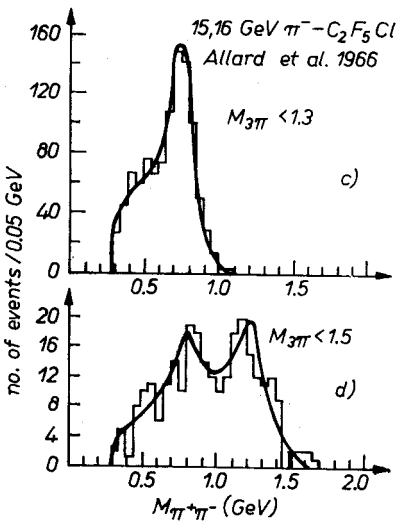

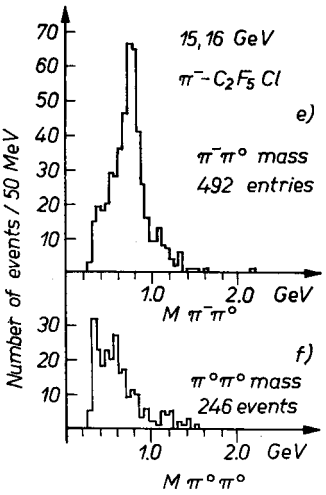

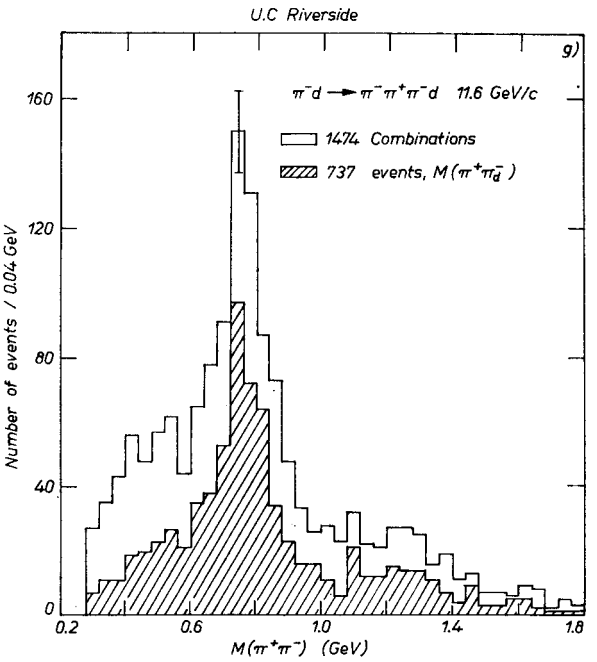

Fig. 4b. π^+d 8.0 (Cnops *et al.* [41]). For 3π mass between 0.85 and 1.45 GeV. Curves are from maximum likelihood fit to Dalitz plot of symmetrized 1^+S and 0^-P; c. π^--Freon 15, 16 GeV (Allard *et al.*, [26]) for $M3\pi < 1.3$ GeV (742 events). The curve includes 80 per cent S wave $\pi\varrho$ and 20 per cent 3π phase space; d. Ditto for $M3\pi > 1.5$ GeV: 267 events. The curve includes 35 per cent ϱ^0, 45 per cent f^0 and 20 per cent phase space; e. Ditto (Daugeras *et al.* [31]) for $\pi^- \rightarrow \pi^-2\pi^0$ (all $M3\pi$) mass $\pi^-\pi^0$ showing $\varrho^-\pi^0$ decay of A_1^-; f. Ditto, mass $\pi^0\pi^0$. Peak near threshold is probably due to small background of events with miss-paired γ's; g. π^-d 11.6 GeV, UC Riverside [42]. The shaded histogram is for the π^- with smaller beam to π^- momentum transfer

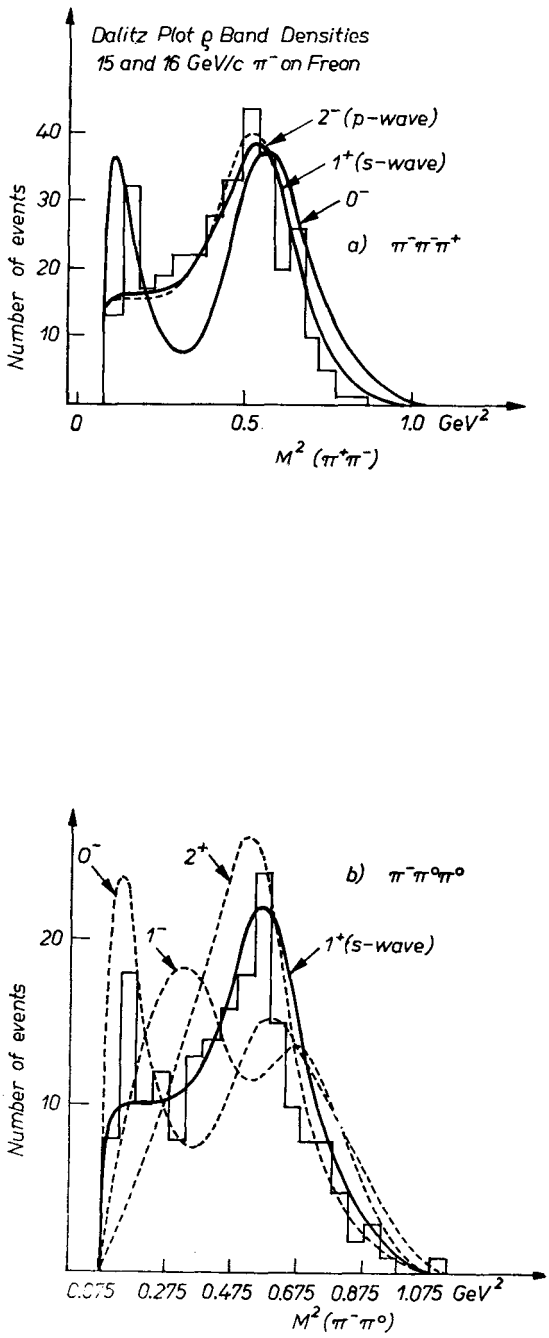

Fig. 5. Example of ϱ band density distribution compared with simplest matrix elements (Zemach [71]) of various J_P; **a.** $M^2\pi^+\pi^-{}_1$, for $0.625 < M\pi^+\pi_2^- < 0.875$ GeV and $1.0 < M3\pi < 1.2$ GeV. Data of Allard *et al.* [26] $\pi^- - C_2F_5Cl$ 15 and 16 GeV (from Veillet [12]); **b.** $M^2\pi^-\pi^0{}_1$, for $0.6 < M\pi^-\pi_2{}^0 < 0.85$ GeV and $0.9 < M3\pi < 1.3$ GeV. Data of Daugeras *et al.* [31]. Figure courtesy Bellini [8]

$J^P_{3\pi}$ either 0^- or 2^- to the dominant 1^+). Note that the admixture is not 1^- if produced by vacuum exchange, not 2^+ or other positive parity because a 3π state of definite parity (+) must yield a symmetric angular distribution even if $\pi\varrho$, $\pi\varepsilon$, *etc.*, are interfering. Alternately, viewed from the ϱ rest system, the asymmetry is explained by a small admixture of S wave $\pi\pi$ (the ε^0) interfering with the dominant P wave (ϱ). If the "bachelor" π is in S wave with respect to the ϱ it must also be in S wave with respect to the ε in order to interfere.

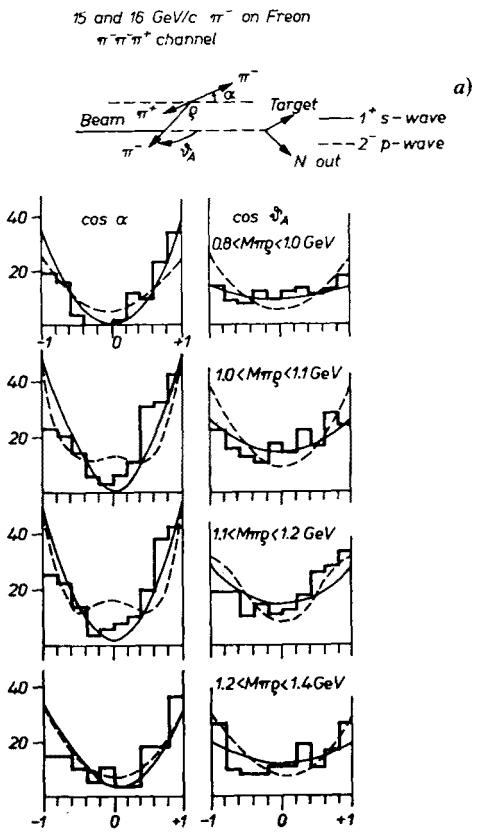

Fig. 6. Examples of $A_1 \rightarrow \varrho\pi \rightarrow 3\pi$ angles, cos θ_n is the polar angle relative to the beam in the 3π rest system, of the normal to the 3π decay plane. Cos θ_A is the bachelor pion's polar angle relative to the beam in the 3πRS, cos α is the polar angle between the π^- of the ϱ (in ϱRS) and the beam in the 3π RS (Adair angle), cos θ_ϱ is corresponding Jackson angle (Beam in ϱ RS); **a.** 15 and 16 GeV π^--freon $\rightarrow \pi^-\pi^-\pi^+$ (Allard *et al.* [26]). The curves show the dominance of 1^+S wave. Note the slight asymmetry in both cos α and cos θ_A distributions indicating *e.g.* admixture of $\pi\varepsilon$ in S wave

Thus the $\varepsilon\pi$ system has $J^P = 0^-$. Similarly if the bachelor π is in D wave the $\varepsilon\pi$ system has $J^P = 2^-$. Similar remarks hold, of course, for the $Q \rightarrow K^*(890)\pi$, *etc.* Fig. 14 shows evidence for coherent production of $\bar{K}q \rightarrow \bar{K}K\bar{K}$ at 12.7 GeV. Other rare channels are listed in Table III.

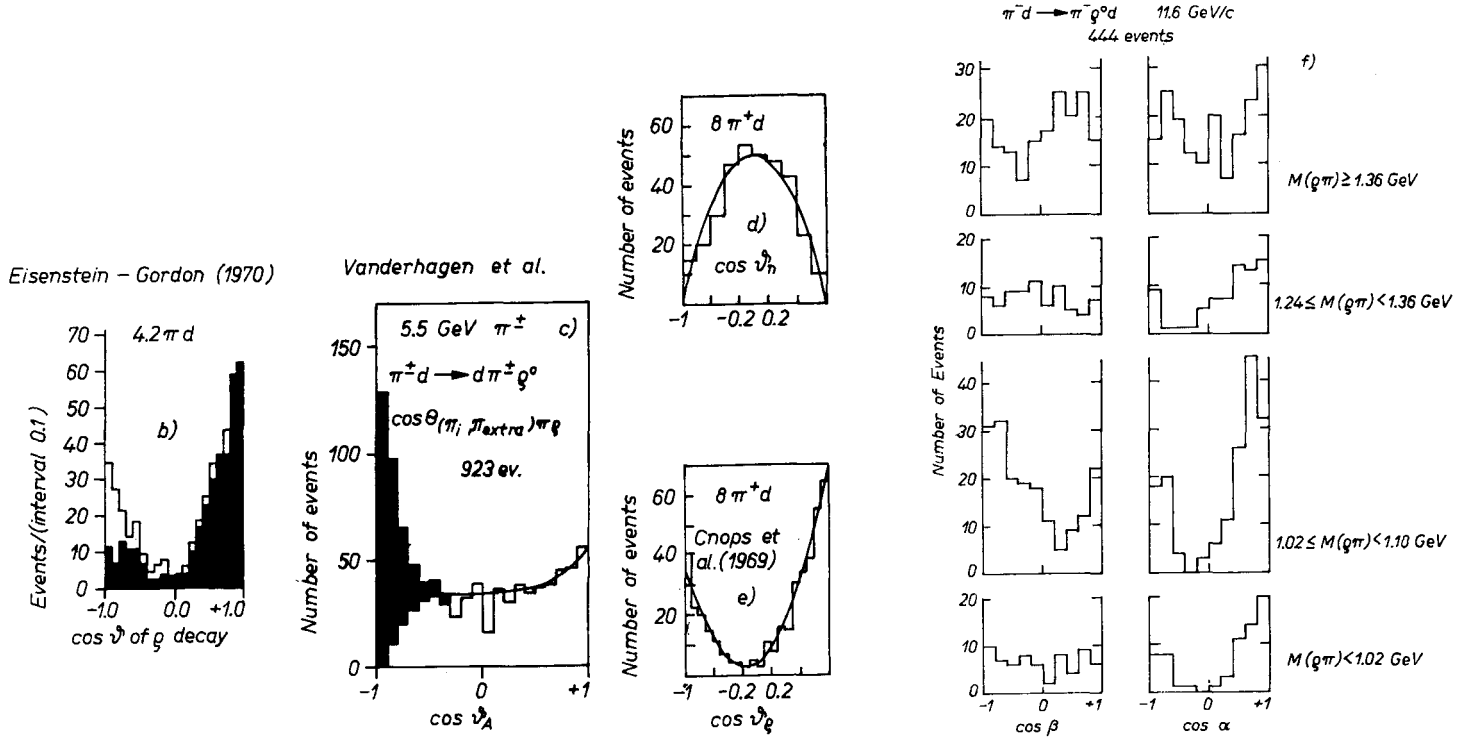

Fig. 6**b**. 4.2 GeV $\pi^+ d$ (Eisenstein and Gordon [34]) cos θ_ϱ. Shaded region is for ϱ's which have smaller beam to dipion momentum transfer; **c**. 5.0 GeV $\pi^\pm d$ (Vanderhaghen *et al.* [36]), cos θ_A. Shaded events are d^*. Solid line is Reggeized OPE prediction — note that it also "explains" the forward asymmetry; **d**. 8 GeV $\pi^+ d$ (Cnops *et al.* [41]) cos θ_n showing nearly pure $\sin^2\theta$; **e**. Ditto, cos θ_ϱ, showing dominance of S wave $\pi\varrho$; **f**. 11.6 GeV $\pi^- d$ (UCR [42]). Here β is θ_p and α is the ϱ helicity angle in the ϱ rest system

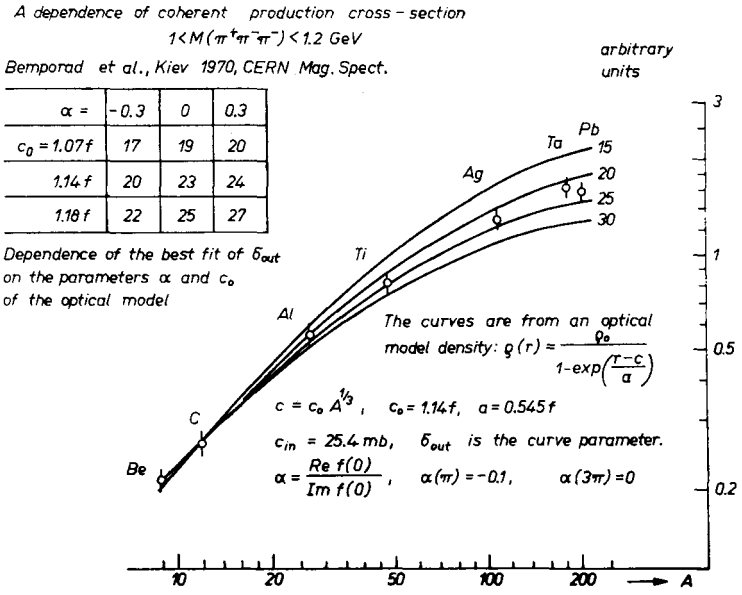

Fig. 7. A dependence of coherent A production cross-section for $1 < M\pi^+\pi^-\pi^- < 1.2$ GeV, π^- 15 GeV (Bemporad *et al.* [46]). α is Re/Im of forward scattering amplitude for A_1, Co is Woods-Saxon radius parameter. Data show that σ_{A_1} is probably $\sim 23 \pm 3$ mb/nucleon at 15 GeV. More recent data (Amsterdam preprint) show that σ_{A_1} may be independent of M_{A_1}, and that $\sigma_{5\pi}$ may be even smaller than σ_π, *i.e.* $\ll 5\,\sigma_\pi$

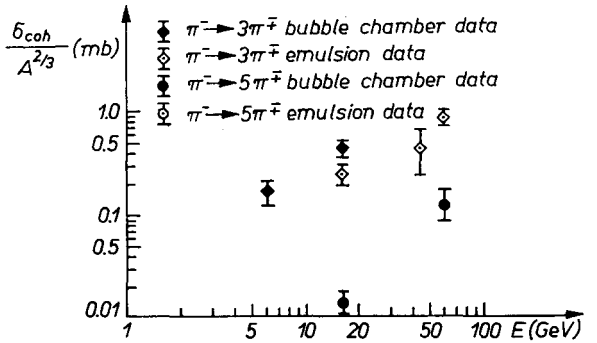

Fig. 8. Energy dependence of $\sigma_{coh}/A^{2/3}$ for $(3\pi)^\pm$ and $(5\pi)^\pm$. From Rybicki [54], showing rising coherent cross-sections. See Mięsowicz [66] for a more recent compilation of emulsion data

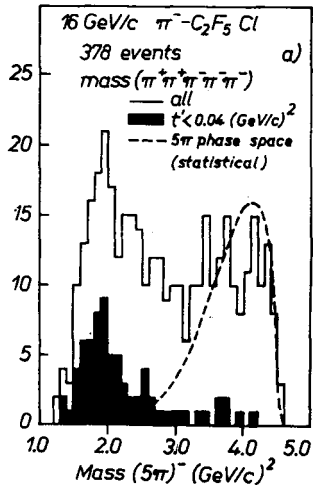

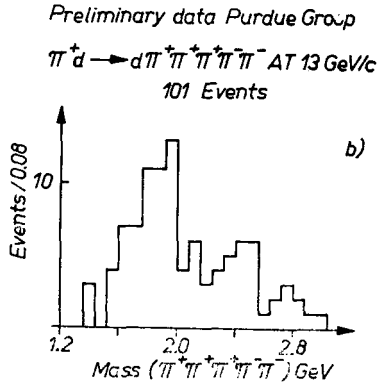

Fig. 9a. 16 GeV π^--$C_2F_5Cl \to 2\pi^+3\pi^-$. Mass 5 π, for all events (solid) and for $t' < 0.04$ (GeV/c)^2 (enriched coherent sample). Dashed curve is statistical phase space. Note peak in $S(1930)$ region. Mass 3π and 2π (not shown) hints of A_1 and ϱ structure. Huson *et al.* [48]; **b.** 13 GeV $\pi^+d \to 3\pi^+2\pi^-d$, Purdue group [45], showing again peaking near $A_1+\varrho$ threshold. Similar 5π mass distributions have been observed by the CERN–ETH–ICL–Milano magnetic spectrometer experiment [46]

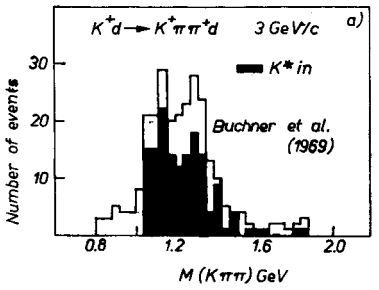

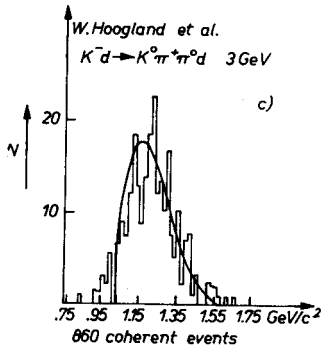

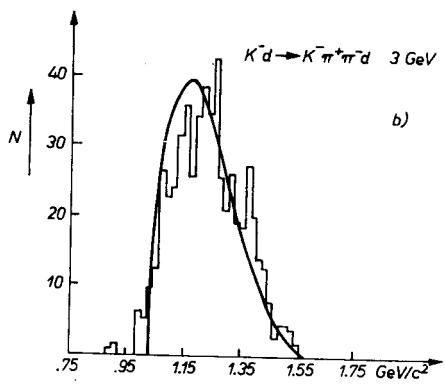

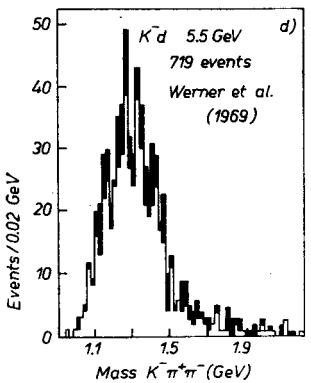

Fig. 10. Examples of $K\pi\pi$ mass distributions. **a.** $K^+d \to K^+\pi^+\pi^-d$ 3 GeV (Buchner *et al.* [58]). Shaded events are for $0.84 < MK\pi < 0.94$; **b.** $K^-d \to K^-\pi^+\pi^-d$ 3 GeV (Hoogland *et al.* [59]). Curve is OPE model of Wolters and De Groot [72] normalized to the total number of events; **c.** $K^-d \to K^0\pi^-\pi^0d$, ditto; **d.** $K^-d \to K^-\pi^+\pi^-d$, 5.5 (Werner *et al.* [61]). d^* in $(Md\pi^- < 2.28$ GeV) are shown shaded

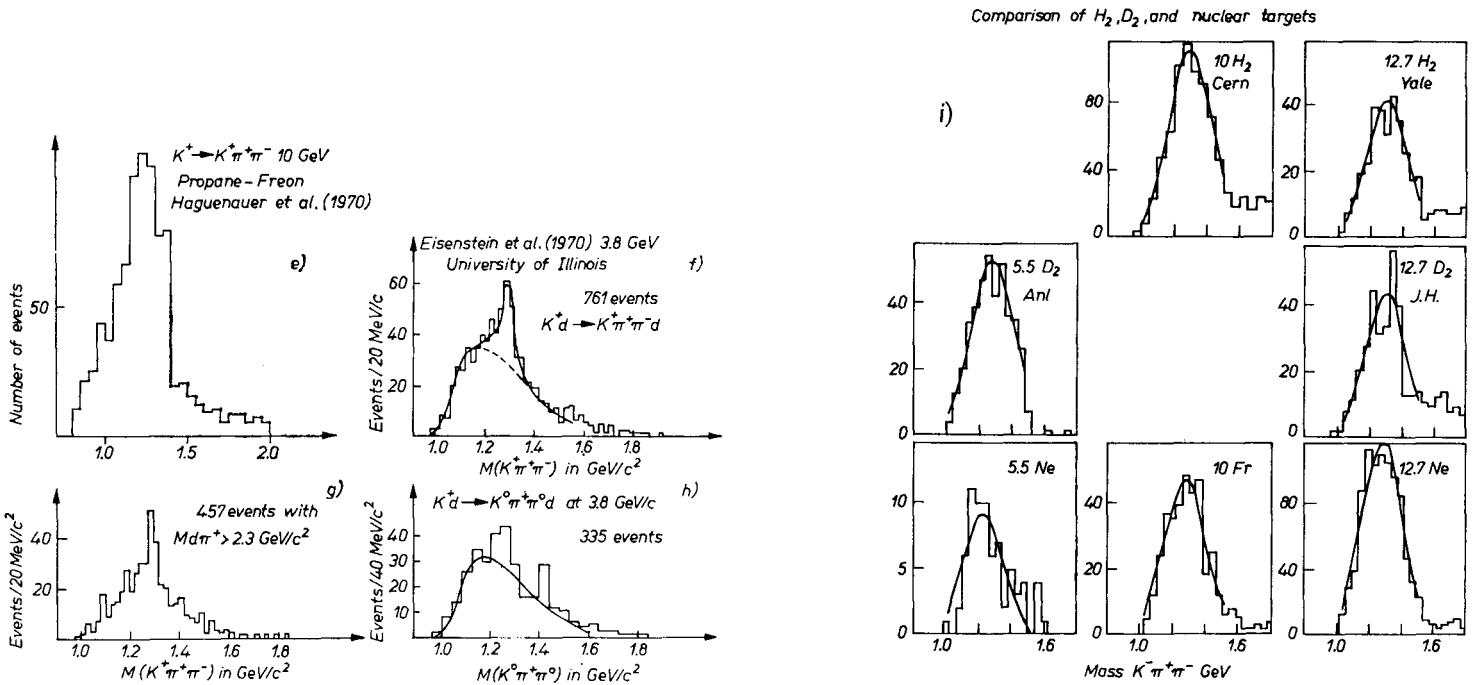

Fig. 10e. K^-—freon→ $K^+\pi^+\pi^-$ (10 GeV) Haguenauer *et al.* [63]. The incoherent background has been subtracted; **f.** $K^+d \rightarrow K^+\pi^+\pi^-d$ 3.8 GeV (Eisenstein *et al.* [60]). The dashed curve shows a Reggeized OPE background. The solid curve is a fit to this ROPE plus a Breit-Wigner of mass 1.30 GeV and FWHM of 54 MeV. More recent plots with about 25% more data are similar; **g.** Ditto with d^* out; **h.** $K^+d \rightarrow K^0\pi^+\pi^0 d$, ditto. Solid curve is ROPE scaled to the data at high and low $K\pi\pi$ mass; **i.** K^-(H_2, d_2, Ne or freon)→ $K^-\pi^+\pi^-$ (ditto), 5.5, 10, 12.7 GeV. $MK^-\pi^+$ between 0.8 and 1.0 GeV was required. From Cnops *et al.* [62]. Curves show the results of fits to the data for $1.0 < M_{K\pi\pi} < 1.5$ GeV of a Gaussian mass distribution with $Mo = 1.3$ GeV and width free, weighted for d_2 and nuclei, by the nuclear form factor squared. The resulting fitted widths were all compatible with 290 MeV (FWHM). See also Fig. 10n

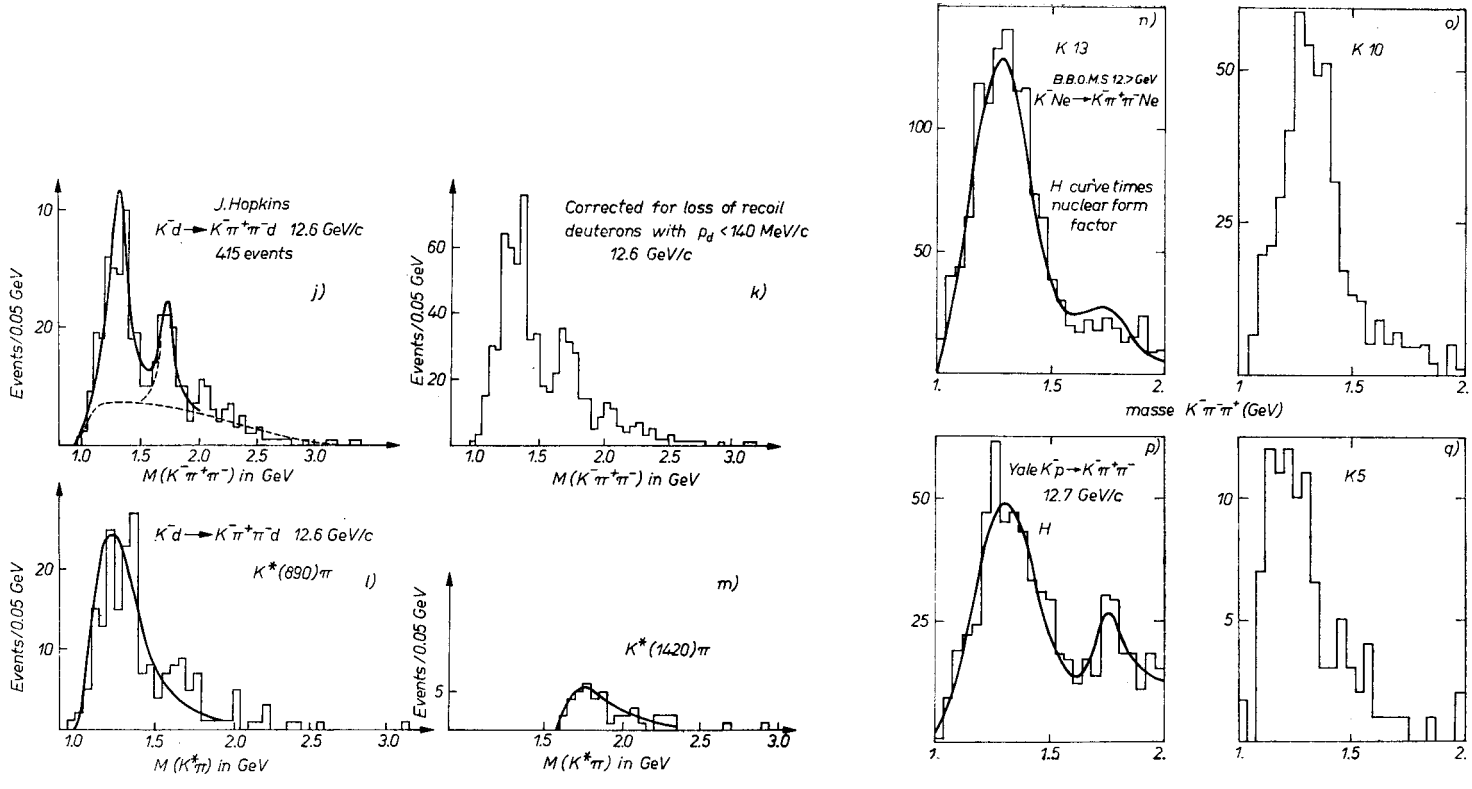

Fig. 10**j**. Antich *et al.* [64]. $K^-\pi^+\pi^-$ mass distribution for the reaction $K^-d \to K^-\pi^+\pi^-d$ at 12.7; superimposed on the background are two Breit-Wigner shapes at 1325 MeV with $\Gamma = 180$ MeV, and at 1740 MeV with $\Gamma = 130$ MeV; **k**. $K^-\pi^+\pi^-$ mass distribution for $K^-\pi^+\pi^-$ final states, corrected for the loss of recoil deuterons with momenta < 140 MeV/c; **l–m**. $K^*(890)\pi$ and $K^*(1420)\pi$ mass spectra from the $K^-\pi^+\pi^-d$ final states; the $K^*(890)$ is defined as: $840 < M(K^-\pi^+) < 950$ MeV and the $K^*(1420)$; $1320 < M(K^-\pi^+) < 1550$ MeV. The curves are calculated according to a diffraction dissociation model with Reggeized pion exchange; **n**, **o**, **q**, $K^-(H_2$ or Ne$) \to K^-\pi^+\pi^-$ (ditto). HLBC $K\pi\pi$ mass spectra at the three energies 5.5, 10, 12.7 GeV; **p**. Mass spectrum from H_2 at 12.7 GeV (Yale group data, quoted by Daugeras [31]) with curve showing fit with two Breit-Wigners (Q and L). This curve, multiplied by the nuclear form factor for Neon is compared with the neon target data in Fig. 10**n**. The agreement is satisfactory

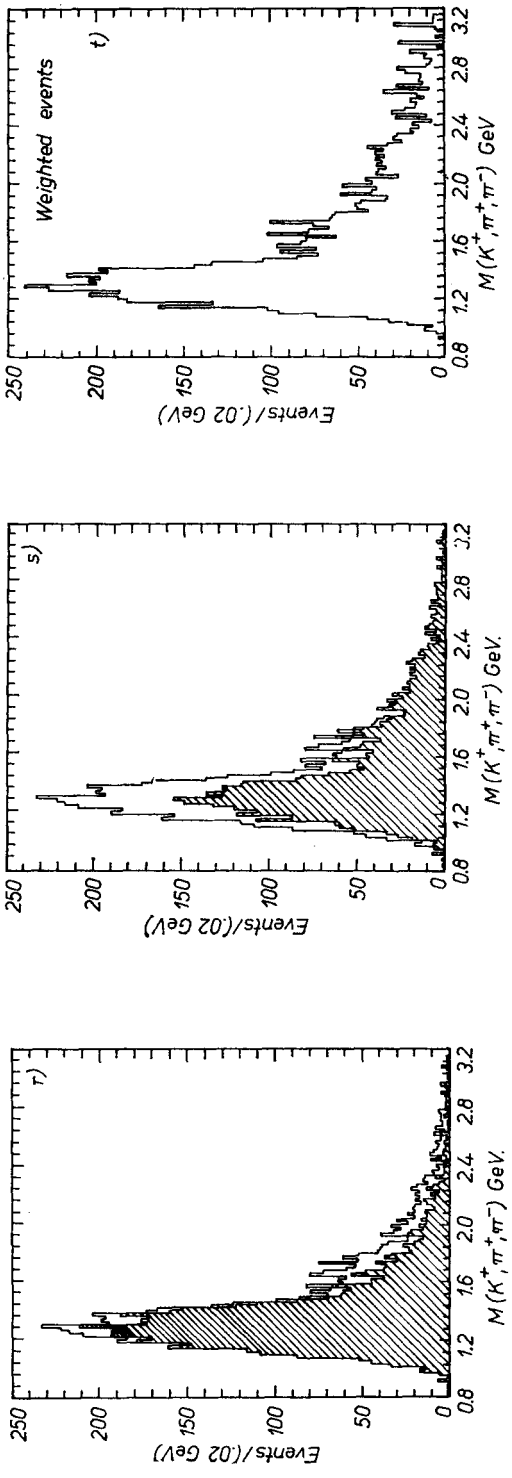
r)
s)
t)
Weighted events
Events/(.02 GeV)
M(K⁺,π⁺,π⁻) GeV.
0
50
100
150
200
250
0.8
1.2
1.6
2.0
2.4
2.8
3.2

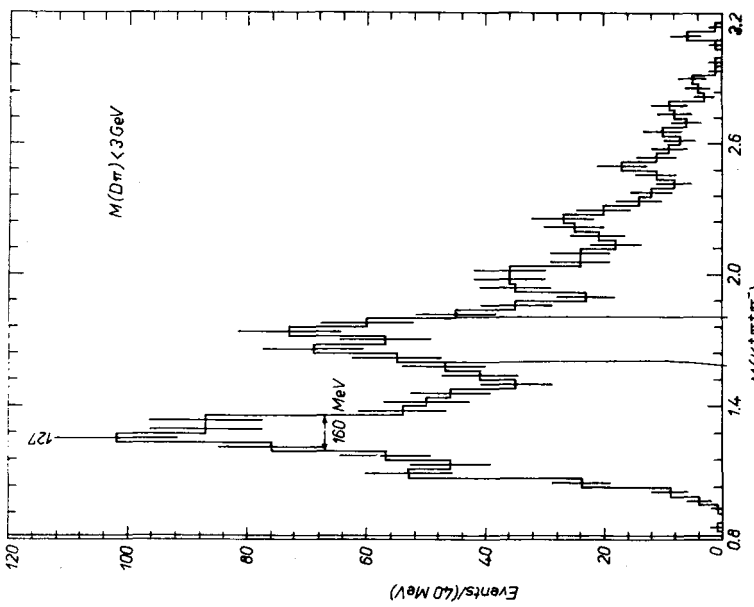

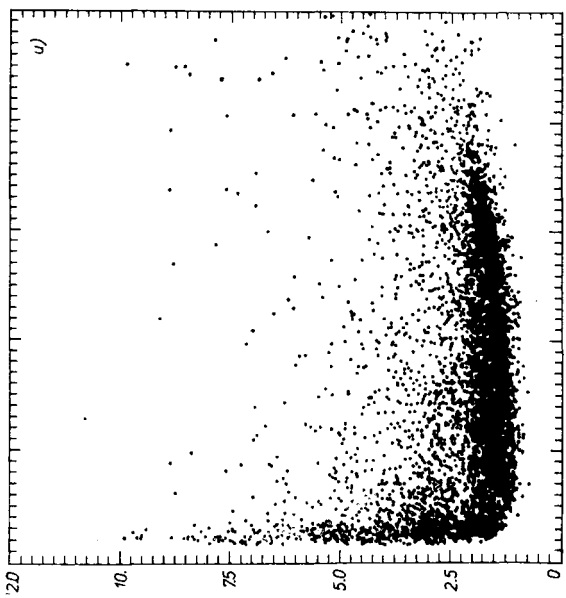

Fig. 10r–v. $K^+d \to K^+\pi^+\pi^- d$, 12.0 GeV, LRL [65] preliminary data with nearly an order of magnitude more coherent events than previous experiments. Fig. 10**r** shows the $K\pi\pi$ mass for all events with d^* out ($M(\pi^+ d) > 2.32$ GeV) shaded. Fig. 10**s** shows it for all events again with 4 prong events shaded showing effect of loss of 3 prong events true of most DBC experiments. Fig. 10**t** shows the effect of weighting by the deuteron form factor. Fig. 10**u** is a scatter plot of $M^2_{d\pi^+}$ *vs* $M^2_{K\pi\pi}$ showing the strong Q and d^* bands and that most of the L signal comes from the overlap region of L and d^* bands. Fig. 10**v** ($M_{K\pi\pi}$ for d^* in $M_{d\pi} < 3$ GeV) shows the same effect: the L signal is strongest in the d^* band. See also Figs 11**h–m**

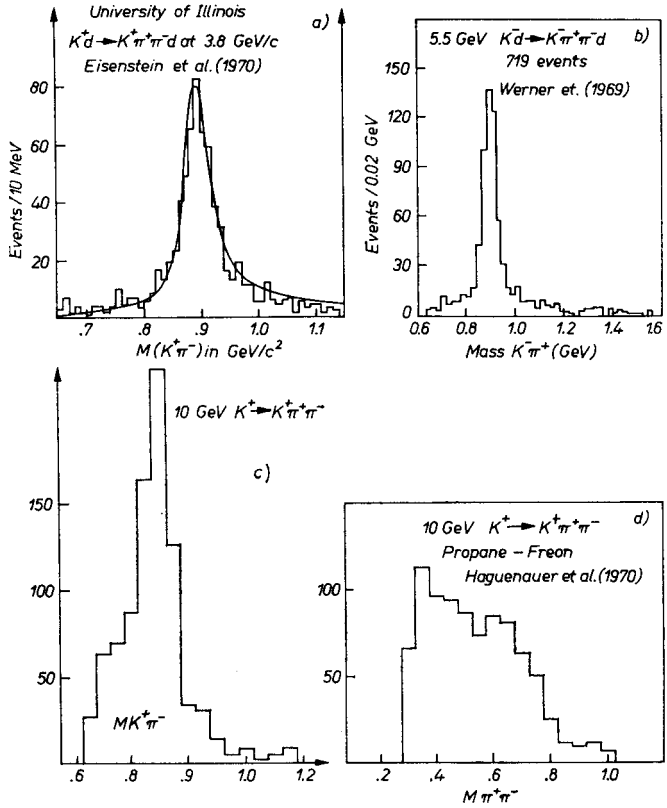

Fig. 11. Examples of $K\pi$ and $\pi\pi$ mass distributions from $K\pi\pi$ final states; **a.** 3.8 GeV/c $K^+d \to K^+\pi^+\pi^-d$, Eisenstein *et al.* [60]. Mass $K^+\pi^-$. Solid curve is K^* Breit-Wigner over phase space background. This fit implies that ~ 90 per cent of the events are associated with $K^*(890)$ production; **b.** 5.5 GeV/c $K^-d \to K^-\pi^+\pi^-d$, Werner *et al.* [61]. Mass $K^-\pi^+$; **c.** 10 GeV K^+—HLBC$\to K^+\pi^+\pi^-$ (Haguenauer *et al.* [63].) Mass $K^+\pi^-$; **d.** Ditto. Mass $\pi^+\pi^-$

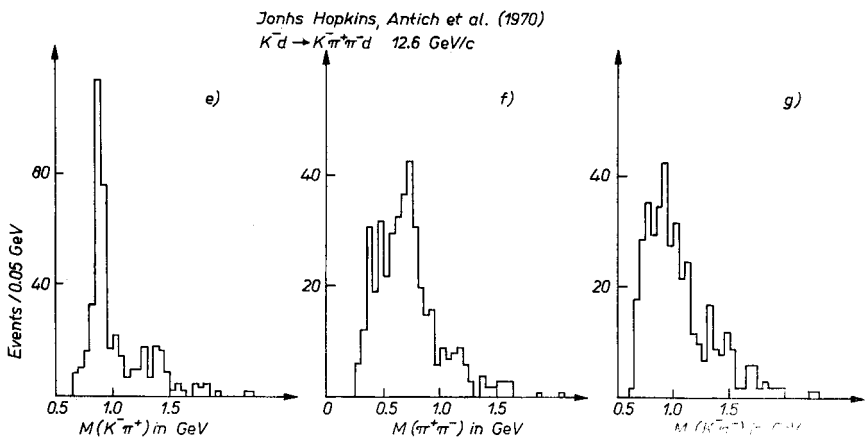

Fig. 11e. 12.7 GeV $K^-d \to K^-\pi^+\pi^-d$ (Antich *et al.* [64]). Mass $K^-\pi^+$ showing signs of $K^*(1400)$ peak as well as $K^*(890)$; **f.** Ditto. Mass $\pi^+\pi^-$ with hint of ϱ^0; **g.** Ditto. Mass $K^-\pi^-$

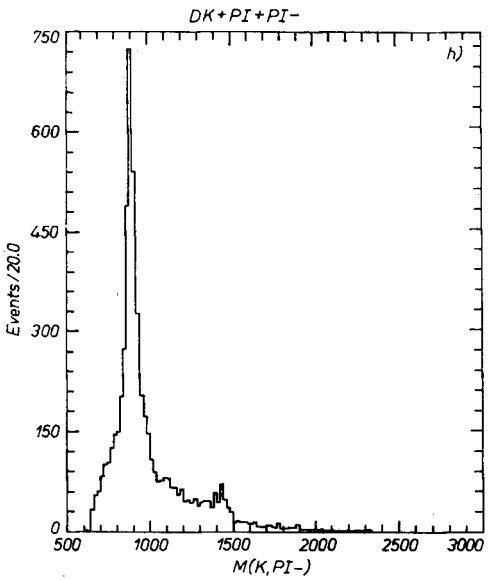
DK+PI+PI-
h)
Events/20.0
M(K,PI-)

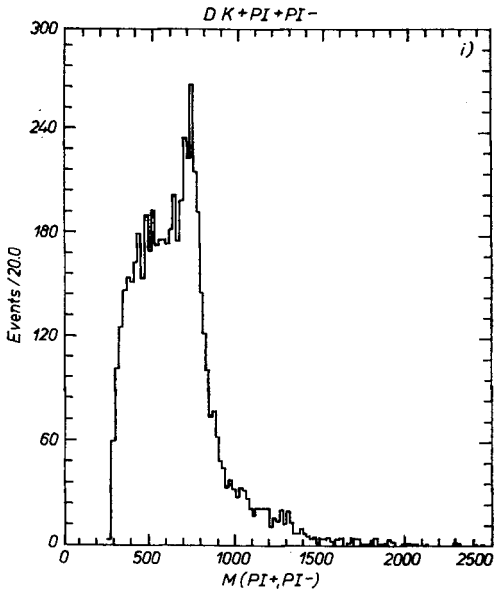
D K+PI+PI-
i)
Events/20.0
M(PI+,PI-)

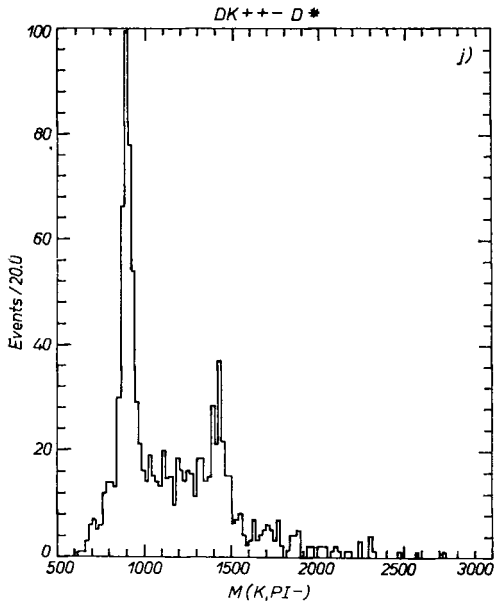
DK++- D*
j)
Events/20.0
M(K,PI-)

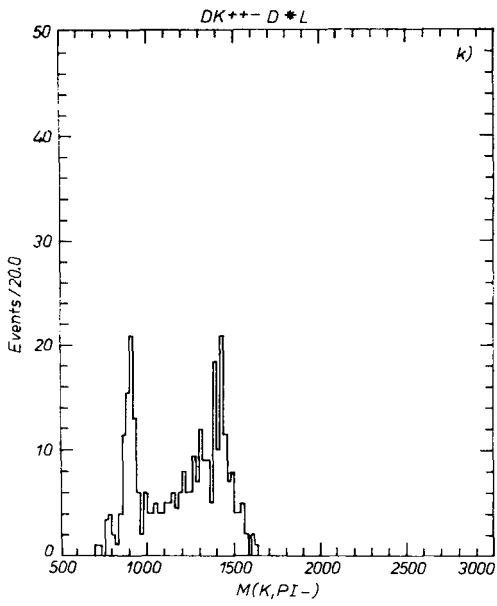

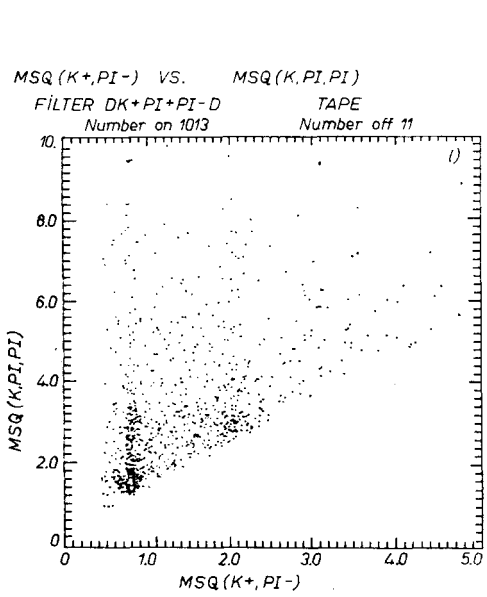

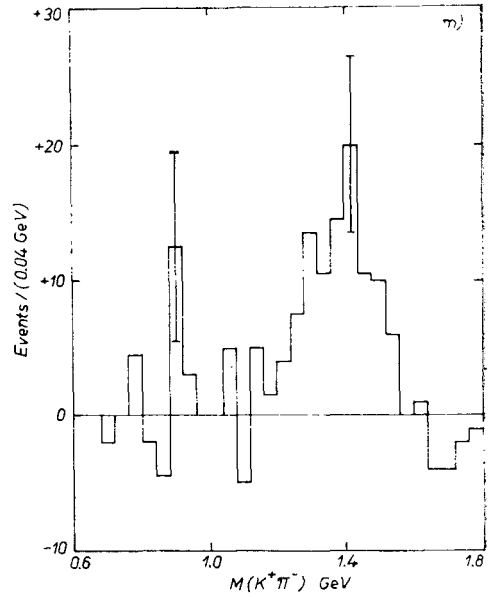

Fig. 11 **h–m.** 12.0 GeV $K^+d \rightarrow \dot{K}^+\pi^+\pi^-d$, LRL [65] preliminary data (corresponding to Figs 10**r–v**). **h.** Mass $K^+\pi^-$, showing $K^*(890)$ and $K^*(1400)$ signals; **i.** Mass $\pi^+\pi^-$ showing some ϱ^0 signal superposed on $K^*(890)$ reflection; very little f^0; **j.** Mass $K^+\pi^-$ for d^* in showing $K^*(1400)$ signal is associated with d^* (as L signal is in Figs 10**u, v**); **k.** Ditto for d^* and L in showing association of $K^*(1400)$ with L (in contrast to Q); **l.** Scatter plot of mass squares $K^+\pi^-$ *vs* $K^+\pi^+\pi^-$ with d^* in showing that $K^*(890)$ signal is strongly associated with Q but not particularly with L while $K^*(1400)$ is associated with L; **m.** Mass $K^+\pi^-$, d^* in, difference of L region and average of mass $K\pi\pi$ regions above and below it, again showing $K^*(1400)$ signal is associated with L region while $K^*(890)$ region is not strongly

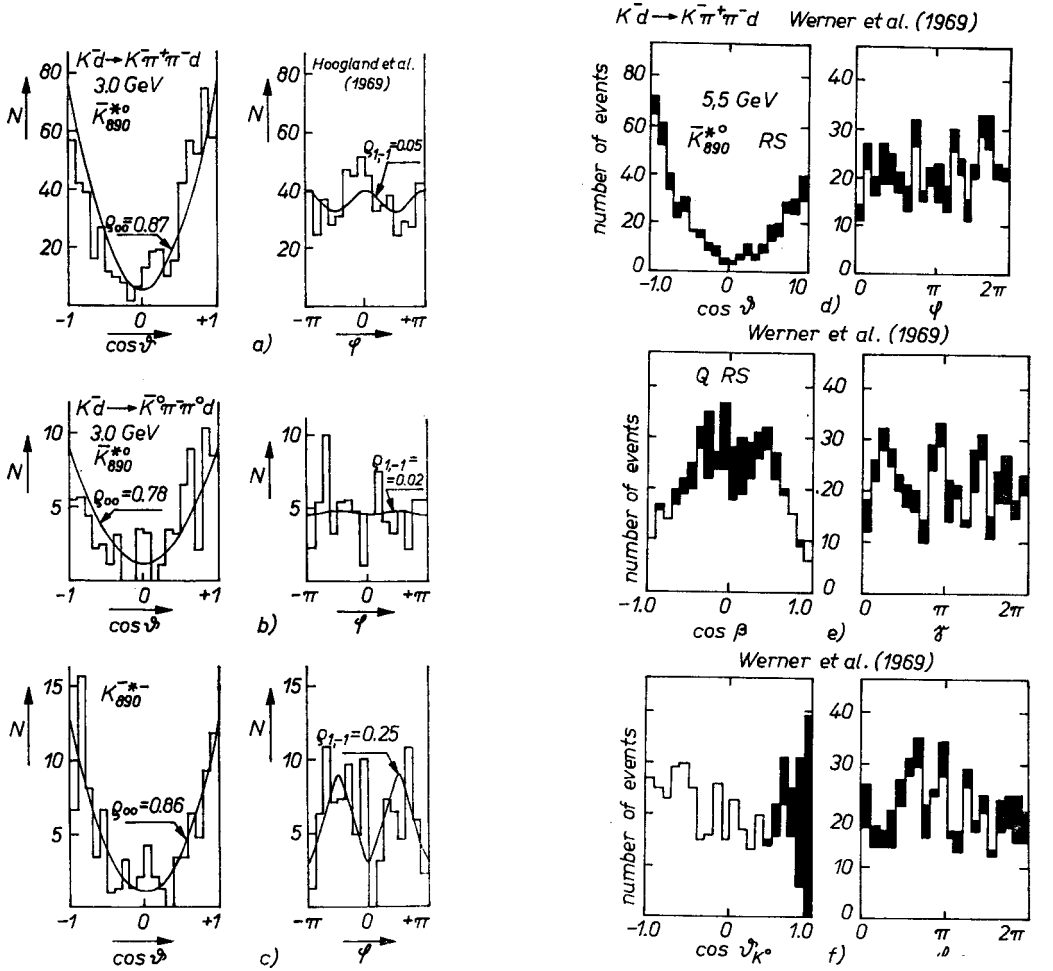

Fig. 12. Examples of angular distributions. **a**. Jackson angles cos θ, φ in $K^{*0}(890)$ RS. $K^-d \to K^-\pi^+\pi^-d$, 3.0 GeV. Hoogland *et al.* [59]; **b**. Ditto for $\bar{K}^{*0}$ from $K^-d \to \bar{K}^0\pi^-\pi^0 d$; **c**. Ditto for $\bar{K}^{*-}$ from $K^-d \to \bar{K}^0\pi^-\pi^0 d$; **d**. Jackson angles in $K^{*0}(890)$ RS, $K^-d \to K^-\pi^+\pi^-d$ 5.5 GeV. Werner *et al.* [61]. Shaded events have $d\pi^-$ mass < 2.28 GeV (d^* in). $K^-\pi^+$ mass between 0.8 and 1.0 GeV and $K^-\pi^+\pi^-$ mass between 1.1 and 1.5 GeV; **e**. Ditto but Jackson angles of $K\pi\pi$ decay plane normal in $K\pi\pi$ RS (QRS); **f**. Ditto but Jackson angles of K^* in QRS

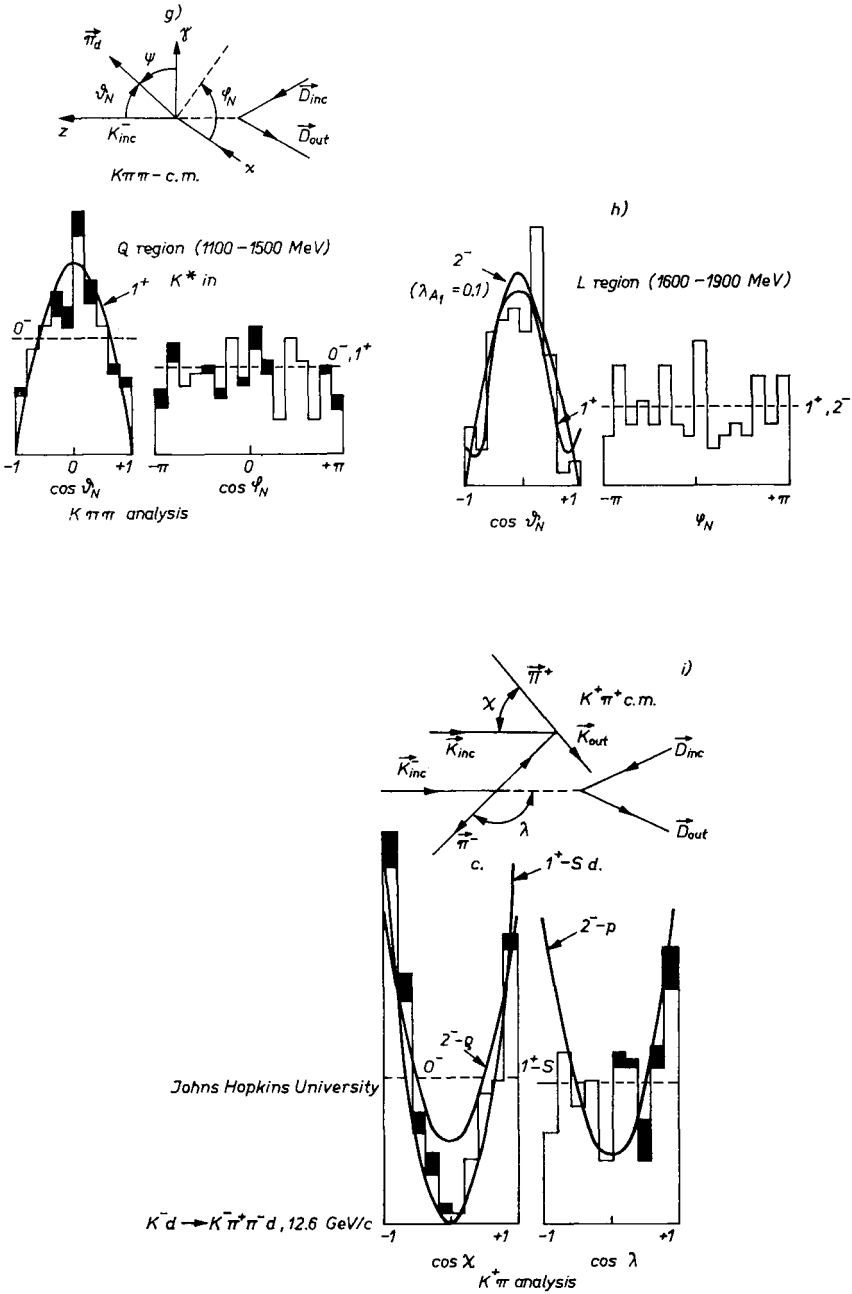

Fig. 12g. Jackson angles Q region 1.1 to 1.5 GeV decay plane normal. $K^-d \to K^-\pi^+\pi^-d$ 12.6 GeV, Antich *et al.* [64], the inset defines the angles. The curves superposed are predictions for various J^P of the Q; **h.** Ditto but for L region (1.6–1.7 GeV in $MK\pi\pi$); **i.** Ditto but Jackson polar angle (X here) of K in the K^* RS, and cos λ = cos of polar angle of bachelor π in QRS. The inset defines the angles. The curves superposed are predictions for various J^P of the $Q \to K^*\pi$ decay

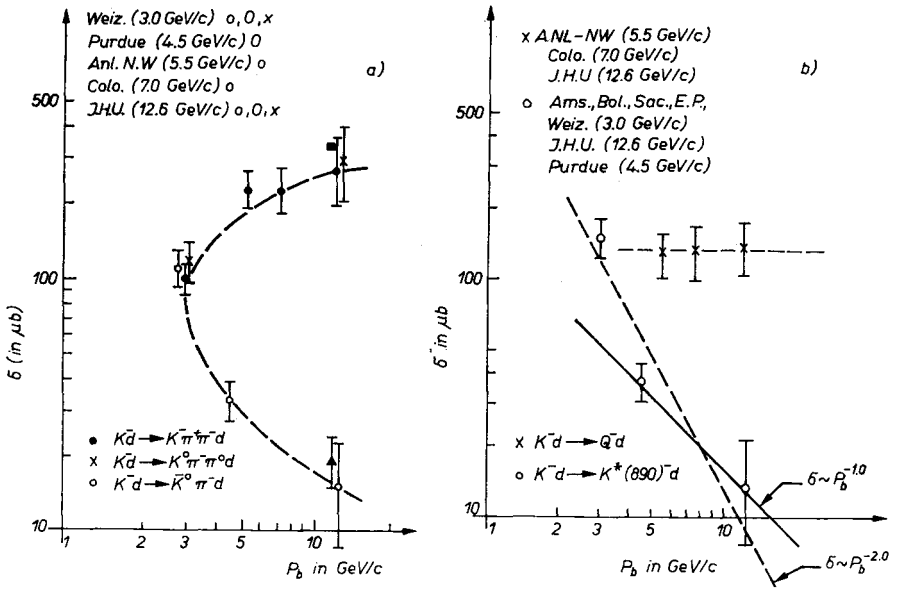

Fig. 13a. Cross-section *vs* beam momentum for $K^-d \rightarrow K^-\pi^+\pi^-d$ (solid dots), $K^-d \rightarrow K^0\pi^-\pi^0d$ (X's) showing that they are approximately equal and rising with P_b as expected for vacuum exchange. The open circles show the cross-section for $K^-d \rightarrow \bar{K}^0\pi^-d$ falling with beam momentum approximately as expected for ω exchange. The black square shows preliminary LRL data [65] at 12 GeV for $K^+p \rightarrow K^+\pi^+\pi^-$ and the black triangle for $K^+p \rightarrow K^0\pi^+d$; **b.** Cross-section *vs* beam momentum for $K^-d \rightarrow Q^-d$ (X's) (approximately independent of beam momentum as expected for vacuum exchange) and for $K^-d \rightarrow \bar{K}^*(890)^-d$ falling roughly linearly with momentum above 4.5 GeV/c. Both of these figures are taken from Antich *et al.* [64], courtesy of A. Pevsner

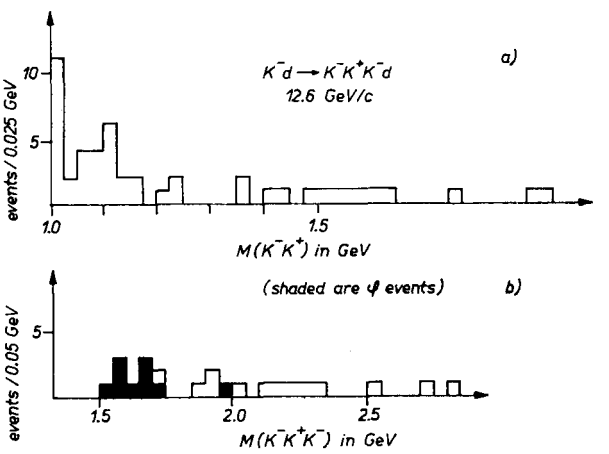

Fig. 14a. K^+K^- mass distribution from $K^-d \rightarrow K^-K^+K^-d$ at 12.6 GeV/c (Antich *et al.* [64]). Note peak in φ (1020) region; **b.** $K^-K^+K^-$ mass distribution. Shaded are φ events

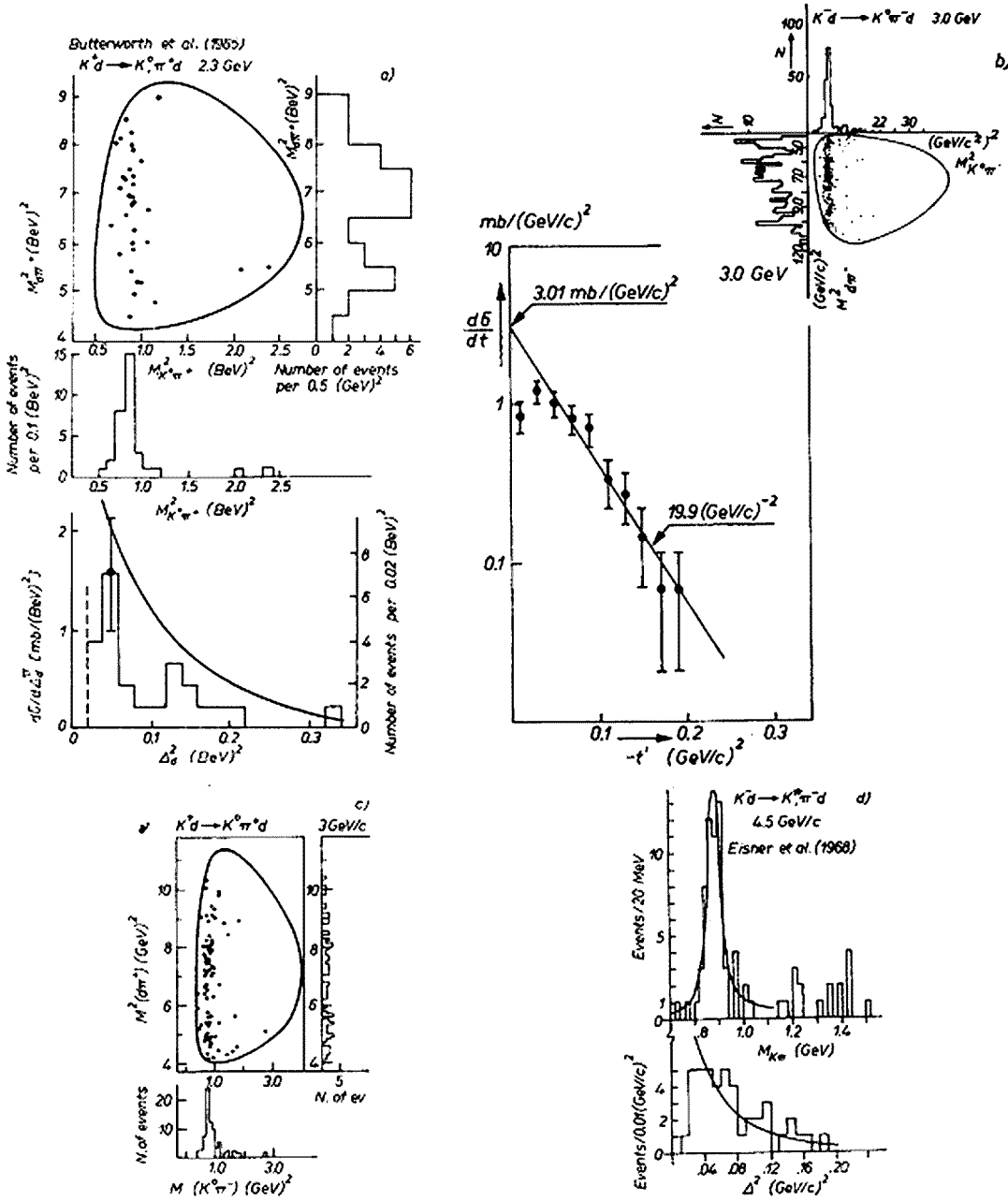

Fig. 15. Typical $K^0, \pi^\pm$ mass or mass squared distributions for $K^\pm d \to K^0_1, \pi^\pm d$. At some beam momenta Dalitz plots and momentum transfer (target to recoil) distributions are shown also. a. K^+d 2.3 GeV, Butterworth *et al.* [57]; b. K^-d 3.0 GeV, Hoogland *et al.* [59]; c. K^+d 3.0 GeV, Buchner *et al.* [58]; d. K^-d 4.5 GeV, Eisner *et al.* [67]. The curve on the $MK\pi$ plot is a simple Breit-Wigner ($M_0 = 885 \pm 5$ MeV, $\Gamma = 55^{-11}_{+10}$ MeV) over background. The curve on the Δ^2 plot is exp $(-6\Delta^2)$ times the square of the deuteron form factor

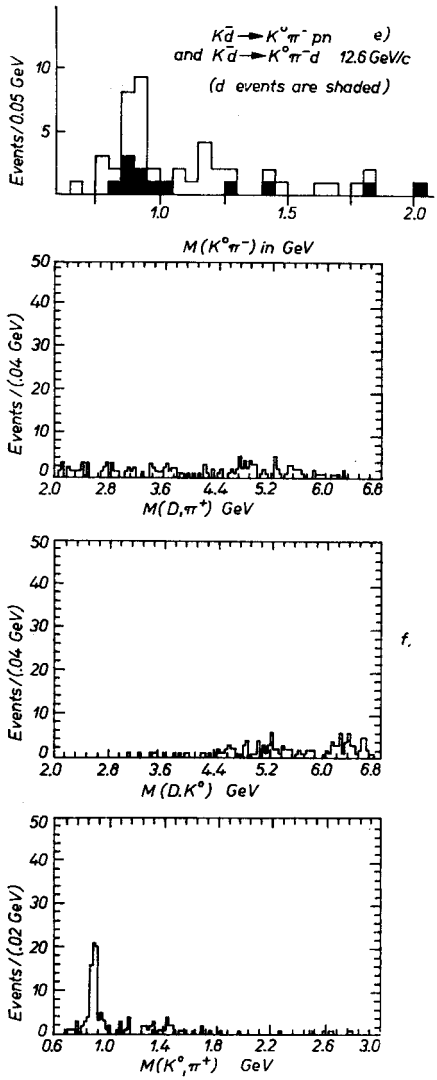

Fig. 15e. K^-d 12.6 GeV, Antich *et al.* [64]. The coherent events are shaded; f. K^+d, 12.0 GeV, LRL [65]. No d^* (or dK^0) peak is apparent here. The $K^*(890)$ signal corresponds to $\sim 20\mu b$ after correcting for other decay modes. The events in the $K^*(1400)$ region correspond to $\sim 5 \pm 5\,\mu b$

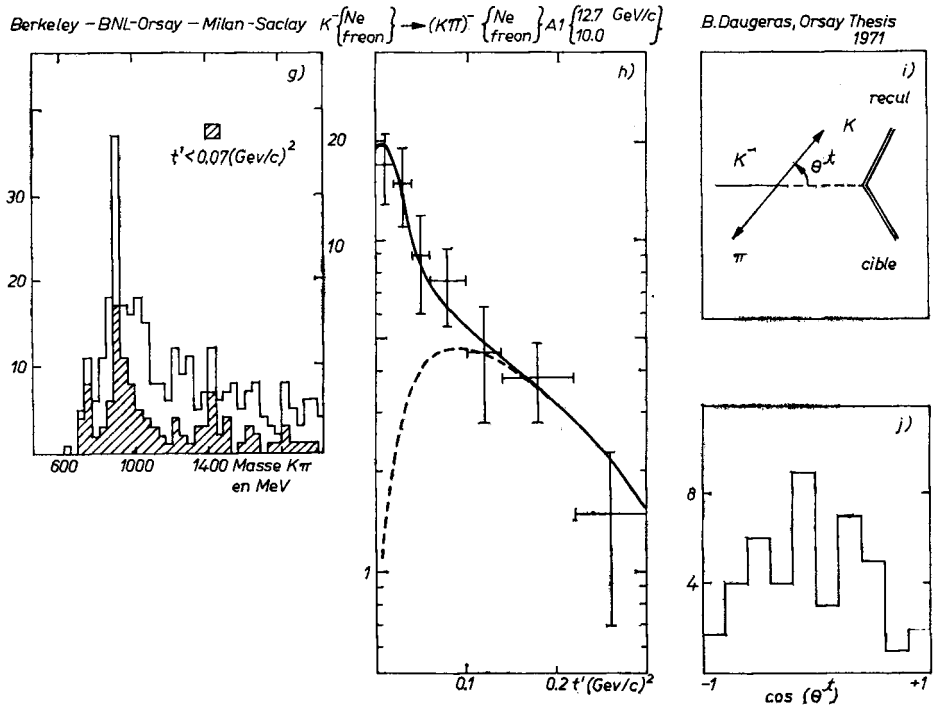

Fig. 15g–j. K^-Ne at 12.7 GeV, Daugeras [31]. $K^0\pi^-$ and $K^-\pi^0$ events both are included in the mass plot (Fig. 15 g), t' (15h) and Jackson angular distribution (Fig. 15j). Fig. 15i illustrates the definition of this angle. The dashed curve in the t' distribution shows the free nucleon distribution which describes the large t' data. The solid curve is a fit to the sum of the dashed curve and a theoretical coherent distribution smeared by experimental resolution. (The zero at $t' = 0$ and the peak at $t' = 0.01$ GeV^2 are obscured by resolution in t' of typically 0.005–0.01 GeV^2. Fig. 15j shows the $\sin^2\theta$ distribution for vector meson production *via* vector exchange

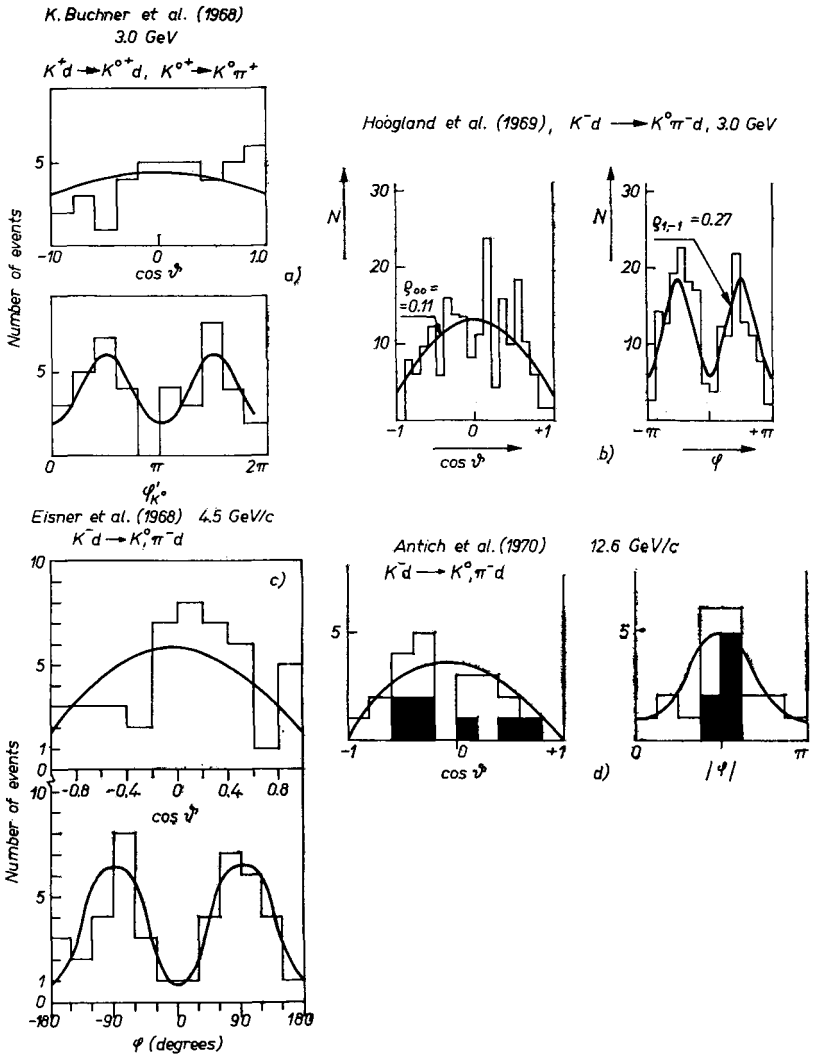

Fig. 16. Typical Jackson angular distributions in $K^*(890)$ RS for $K^{\pm}d \to K_1^0\pi^{\pm}d$; **a.** K^-d 3.0 GeV/c, Buchner *et al.* [58]. The curves are calculated for $\varrho_{00} = 0.26$, $\varrho_{1-1} = 0.27$, Re $\varrho\,10 = 0.04$. The K^* is defined as 0.82 to 0.94 GeV in $MK\pi$; **b.** K^-d 3.0 GeV, Hoogland *et al.* [59]; **c.** K^-d 4.5 GeV, Eisner *et al.* [67]. The curves are calculated for $\varrho_{00} = 0.12$, $\varrho_{1-1} = 0.38$, Re $\varrho 10 = 0.04$; **d.** K^-d 12.6 GeV, Antich *et al.* [64]. The coherent events are shaded. The solid curves represent the predicted distributions for $K^*(890)$ production *via* ω exchange with no absorption and no deuteron spin flip

8. ω^0 exchange processes

The coherent reaction $K \to K\pi$, which cannot proceed *via* 0^+ exchange but can go *via* higher natural parity exchange, *e.g.* $1^-(\omega^0)$, (and which must vanish in the forward direction if proceeding *via* natural parity exchange) has been observed at several beam momenta in DBC experiments and now also from neon at 12.7 GeV/c in both $K^0\pi^-$ and $K^-\pi^0$ modes (see Table IV). Fig. 13 shows that, in contrast to the slowly rising $K \to K\pi\pi$

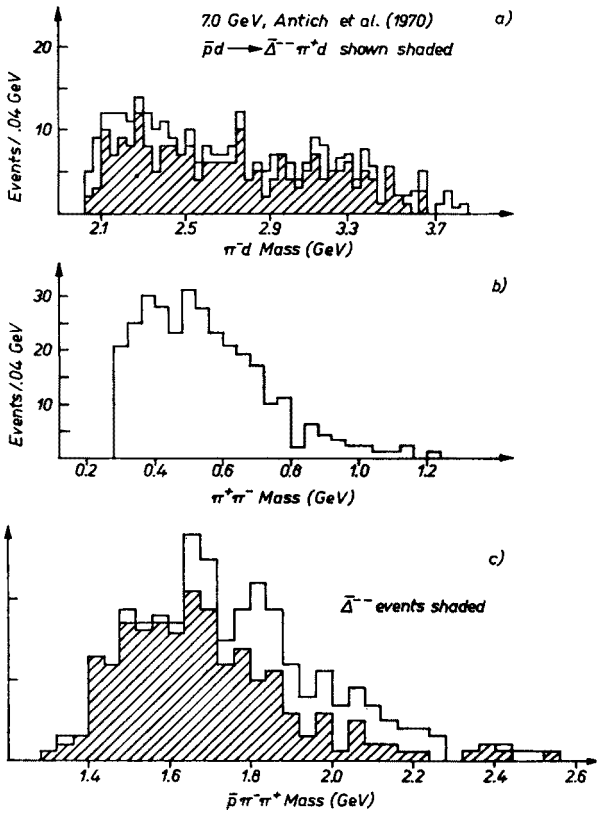

Fig. 17**a**. Mass $\pi^- d$ distribution for $\bar{p}d \to \bar{p}\pi^-\pi^+ d$ at 7.0 GeV. Antich *et al.* [64]. $\bar{\Delta}^{--}\pi^+ d$ events are shaded; **b**. Ditto, $\pi^+\pi^-$ mass; **c**. Ditto, $\bar{p}\pi^-\pi^+$ mass

coherent production cross-section (and roughly constant at 140μb/dQ region coherent production cross-section), the $K \to K\pi$ cross-section falls rapidly to ~20μb at 13 GeV (and the $K^*(890)$ perhaps linearly with beam momentum as expected for ω exchange). That the $K^*(890)$ dominates $K\pi$ mass spectra is shown in Fig. 15 and Fig. 16 shows that the K^* Gottfried-Jackson angular distributions are compatible with those expected for $0^- \to 1^-$ *via* vector exchange (with no deuteron spin flip), *i.e.* $\sin^2\theta$ and $1-2\varrho_{1-1}\cos 2\varphi$ with $\varrho_{11} \approx |\varrho_{1-1}| \approx 0.5$.

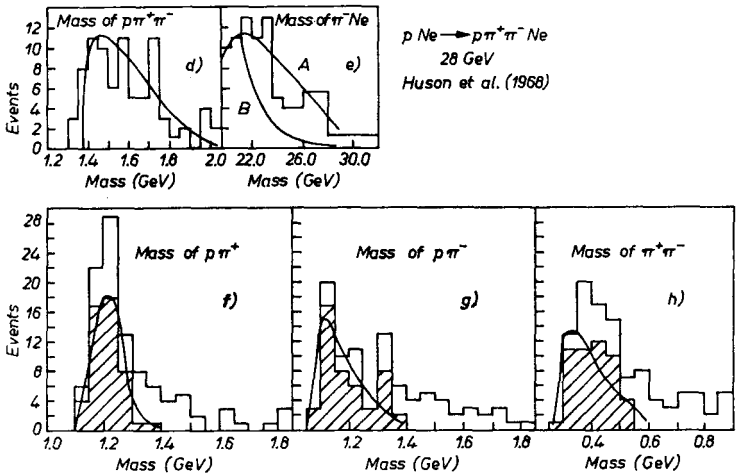

Fig. 17**d**. Mass $p\pi^+\pi^-$ for $p\mathrm{Ne} \rightarrow p\pi^+\pi^-$ Ne at 28 GeV. Huson, Miller and O'Neal [70]. The curves are Berger's Reggeized OPE prediction. Lack of agreement of the low end of the spectrum is due to Berger's zero width assumption for Δ^{++}; **e**. Ditto, mass π^-Ne for $p\pi^+\pi^-$ mass less than 1.6 GeV. Curve *A* is Berger's prediction. Curve *B* is his prediction with the subenergy dependence omitted for Pomeron exchange; **f**. Mass $p\pi^+$. The shaded areas are for $p\pi^+\pi^-$ mass < 1.6 GeV. The curves are phase space for $\Delta^{++}\pi^-$ decay given the observed $p\pi^+\pi^-$ mass distribution below 1.6 GeV (Fig. 17**d**); **g**. Mass $p\pi^-$ ditto; **h**. Mass $\pi^+\pi^-$ ditto

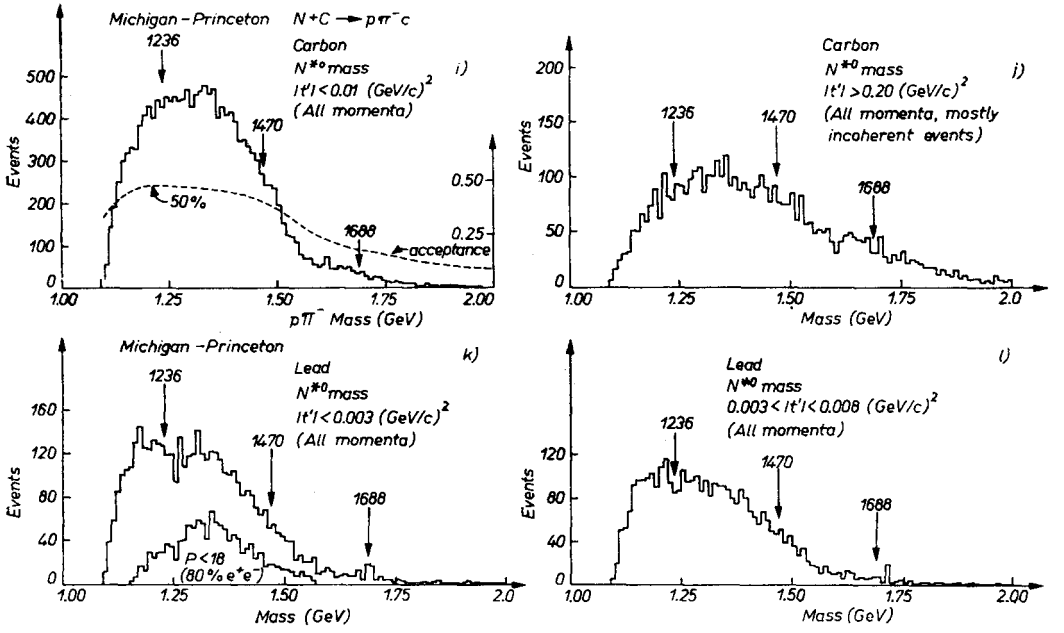

Fig. 17**i–l**. Mass $p\pi^-$ for $nA \rightarrow p\pi^-A$, Michigan-Princeton [71] preliminary data from carbon (**i, j**) and lead (**k, l**). Figs **i, k** are for events in the coherent peak; Figs **j, l** for incoherent events. No signs of N^* observed in π^-p scattering are apparent. Again a diffractive peak starting near threshold (here at $m_p + m_\pi$) and a few hundred MeV wide, is observed

The possible contribution of Coulomb production to coherent K^* production should rise with beam momentum and Z. It should be less than 2 μb (*i.e.* a few % of the coherent production cross-section) for 12.7 GeV/c $K\pi^-$ neon, but it may be observable from heavy elements at CERN and BNL energies.

Recall that $K \to K\pi$ does not require G exchange. However, $\pi^\pm \to \pi^\pm\pi^0$ does, but has not so far been observed due to the enormous background of elastic πp and πd scatters when the π^0 decay γ's are not observed.

Fig. 19, however, shows evidence [73] for $\pi^+ \to \pi^+\pi^+\pi^-\pi^0$ coherent production at 11.7 GeV, with a surprisingly large cross-section (180 μb/d!). If ω^0 exchange is responsible,

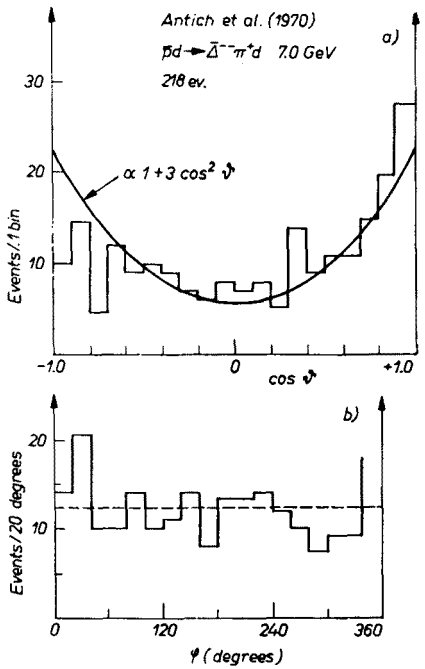

Fig. 18. Jackson angular distribution for $\bar{\Delta}^{--}$RS, $\bar{p}d \to \bar{\Delta}^{--}\pi^+d$ 7.0 GeV. Antich *et al.* [64]. The curves show the $1+3\cos^2\theta$, flat φ distributions expected for a $\bar{\Delta}^{--}$ aligned in an $m = \pm{}^1/_2$ state

and if the produced states are not too heavy, the cross-section should rise nearly linearly as p_b is decreased, *i.e.* this channel should remain comparable to $\pi d \to 3\pi d$ at lower beam momenta. Fig. 19**d** ($M_{4\pi}$) shows what may be a series of superposed diffractive peaks corresponding to quasi-2-body channels $\pi\omega$, $\varrho\varrho$, πA_1, *etc.* More data is available in existing DBC film on this and other ω exchange channels (*e.g.* $K \to K\pi$) and should be published!

Note that $\pi \to 4\pi$ does not have to vanish in the forward direction if the 4π system has unnatural parity (and is produced by natural parity exchange), in contrast to 2π (and $K\pi$) which can have natural parity only.

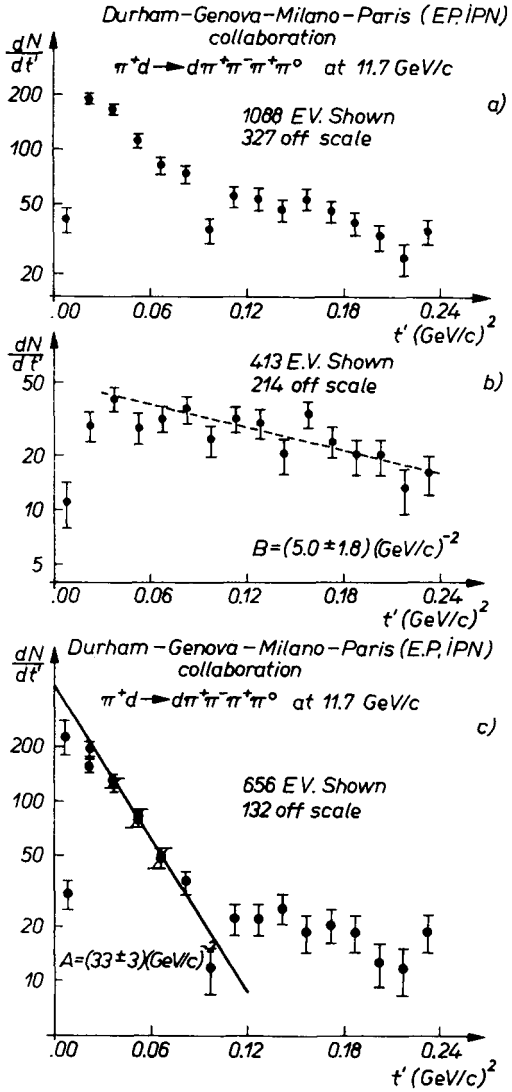

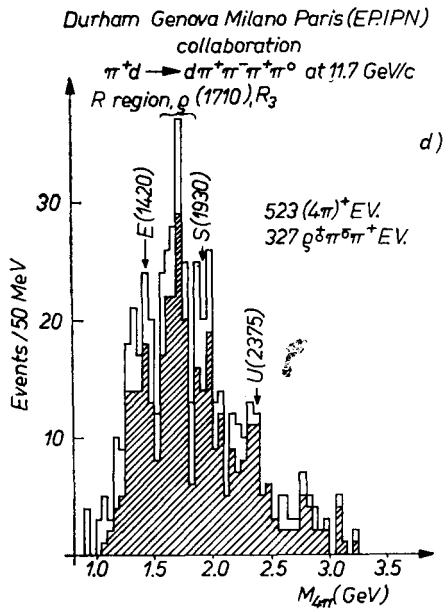

Fig. 19. t' distributions for reaction $\pi^+d \rightarrow d\pi^+\pi^-\pi^+\pi^0$ at 11.7 GeV/c. **a.** All events (1415); **b.** 627 ambiguous events (to calculate the slope, the first two points were not taken into account); **c.** 788 uniquely identified events. Open points are uncorrected. Full points are corrected for the visibility cut of the deuteron assumed to be identical to that experimentally found for the reaction $\pi d \rightarrow 3\pi d$. Full line is the best fitted exponential coming from that reaction; **d.** $M_{4\pi}$ mass distribution for the $(4\pi)^+$ system: 523 events with $t' < 0.12$ (GeV/c)^2. Hatched histogram: 372 events in which at least one $(\pi\pi)$ combination lies in the ϱ band (620–900 MeV)

9. Conclusions

Remarkable similarities are becomin gapparent among the dominant coherent processes $\pi \to 3\pi$, $K \to K\pi\pi$, $n \to n\pi\pi$:

1. The cross-section for a particular process (*e.g.* $\pi^+ \to A_1^+$, $K^- \to Q^-$) is roughly independent of beam momentum (Fig. 13), while coherent cross-sections for a topology (*e.g.* $\pi \to 3\pi$, $K \to K\pi\pi$) rise with beam momentum (Figs 8, 13). Typical particular coherent cross-sections are of order 1 per cent of the beam-nucleus total cross-section.

2. Each coherently produced topology's mass distribution seems to show the beginning of what is probably a series of broad (a few hundred MeV wide) peaks, the first peak somewhat above the threshold mass for the least massive quasi-two-body state out of which the topology can be made (*e.g.* the $A_1(1070)$ peak near $\varrho+\pi$ threshold, $Q(1300)$ near $K^*(890)+\pi$, $N^*(1470)$ near $\Delta(1238)+\pi$), the next peak just above the next threshold (*e.g.* $A_3(1640)$ near $f^0+\pi$, $L(1780)$ near $K^*(1400)+\pi$). Sometimes the bumps probably overlap (*e.g.* $K^*(890)\pi$, $K\varrho$ in $Q(1300)$).

3. The peaks apparently are not shaped exactly like a "normal" (Jackson 1964) Breit-Wigner.

4. The spin and parity (J^P) of each peak seems to correspond to that obtained by combining in relative S wave ($l = 0$) its least massive possible quasi-two-body constituents (*e.g.* $\varrho(1^-)+\pi(0^-) \to A_1(1^+)$, $K^*_{890}(1^-)+\pi(0^-) \to Q(1^+)$, $f^0(2^+)+\pi(0^-) \to A_3(2^-)$, $K^*_{1400}(2^+)+\pi(0^-) \to L(2^-)$). The "decay back" (*e.g.* $A_1 \to \varrho+\pi$) probably is a mixture of S and D waves, however, and the heavier objects can be expected to have many "decay" modes.

5. Each prominent peak seems to be produced aligned only in those states permitted by "elementary vacuum" ($J^P = 0^+$) exchange (*e.g.* π, K beams ($J^P = 0^-$) produce the A_1, Q, probably also A_3, L, aligned with $m = J_Z = 0$ and $N \to N^*(1470)$ is produced with $m = \pm 1/2$). The distribution of the azimuthal angle around the exchanged particle (Treiman-Yang angle) is roughly flat.

6. The A dependence of the coherent production cross-section implies that the outgoing state (at least the A_1 and Q) is absorbed in nuclear matter with cross-section roughly equal to that of the beam particle, rather than roughly equal to the sum of its quasi-two-body constituents (*e.g.* $\sigma_{A_1} = 23 \pm 3$ mb $= \sigma_\pi < \sigma_\pi + \sigma_\varrho \approx 45$ mb).

7. In addition to the dominant processes, several rarer but apparently similar processes have been observed, *e.g.* $K \to K\varphi$, $\pi \to 5\pi$ (mass 5π peaks near $A_1+\varrho$ threshold and probably also has absorption cross-section $\approx \sigma_\pi \ll 5\sigma_\pi$). Coherent production of $K3\pi$ states is observed with cross-sections roughly an order of magnitude smaller than for $K2\pi$.

Characteristics 1, 2, 4, 5 are expected for states coherently produced *via* vacuum exchange with the nucleus.

Besides these dominant vacuum exchange processes there is some evidence for another class of processes showing the characteristics expected for ω^0 exchange notably $K \to K\pi$.

1. The cross-section for a particular process (*e.g.* $K \to K^*(890)$) falls with increasing beam momentum roughly as $1/p_b$ (Fig. 13) and the topological cross-section probably more slowly.

2. The $K^*(890)$ is produced aligned in an $m = \pm 1$ state and its Treiman-Yang angular distribution is compatible with that expected for vector exchange. At lower energies the situation may be more complicated.

3. There is evidence from one experiment for the existence of coherent $\pi \to 4\pi$ production from deuterium.

The clearest conclusion is that more data is needed! Note, for example, that there is no published $\pi^- d$ data above 5.1 GeV, nor $K^+ d$ above 3.8, no pd at all, no He at all, very little information on channels involving π^0's. Any such new data should teach us something!

In addition to my colleagues at Berkeley and at the several labs collaborating with us on HLBC experiments (and Theorists at these places) who have corrected my misconceptions on many points I want to thank the participants in this year's Cracow summer school, especially A.S. Goldhaber, A. Białas and T.H. Bauer for several clarifying comments during these lectures. I am grateful to the school's organizers and to the UC Berkeley research committee for support in Poland and travel to and from, respectively, which together made it possible for me to give the lectures.

REFERENCES

[1] H. H. Bingham, CERN/D.Ph.II/PHYS/70–60, published in *Proceedings of the Topical Seminar on Interactions of Elementary Particles with Nuclei*, Trieste 1970, ed. G. Bellini, L. Bertocchi and S. Bonetti, p. 37.

[2] J. D. Jackson, *Rev. Mod. Phys.*, **42**, 12 (1970).

[3] B. Margolis, *Trieste Conf.* 1970 (see Ref. [1]).

[4] R. J. Glauber, in *High Energy Physics and Nuclear Structure*, ed. G. Alexander (North Holland, Amsterdam 1967), p. 311; *High Energy Physics and Nuclear Structure*, ed. S. Devons (Plenum Press, New York 1970), p. 207; *Lectures in Theoretical Physics*, ed. W. E. Brittin *et al.* (Interscience, New York 1959), Vol. I, p. 315.

[5] a) L. Stodolsky, *Phys. Rev.*, **144**, 1145 (1966).
b) M. Ross, L. Stodolsky, *Phys. Rev.*, **149**, 1172 (1966).

[6] J. S. Trefil, *Phys. Rev.*, **180**, 1366 (1969); also *Nuclear Phys.*, **B11**, 330 (1969); J. S. Trefil, *Phys. Rev. Letters*, **23**, 1075 (1969).

[7] D. Fournier, *Reactions de Production Coheréntes, Orsay Internal Report* L.A.L. 1237 and *Thèse Université*, Paris-Sud 1971.

[8] G. Bellini, *Herceg-Novi School*, 1969, Strasbourg—Belgrade.

[9] P. Franzini, in *Proceedings of the Stony Brook Conference on High Energy Collisions*, ed. C. N. Yang *et al.* (Gordon and Breach, New York 1969).

[10] L. de Lella, in *Proceedings of the Lund Conference on Elementary Particles*, ed. G. von Dardel (Berlingska Boktryckeriet, Lund 1969).

[11] O. Czyżewski, in *Proceedings of the XIVth Conference on High Energy Physics*, Vienna 1968.

[12] J. J. Veillet, in *Proceedings of the CERN Conference on High Energy Collisions of Hadrons*, 1968, CERN 68–7.

[13] C. Fisher, *Herceg-Novi School*, 1965, Strasbourg—Belgrade.

[14] S. Ting, *Trieste Conf.* 1970 (see Ref. [1]), *Vienna Conf.* 1968 (see Ref. [11]).

[15] D. Leith, *Scottish Universities Summer School* 1970, and *SLAC Report.*

[16] D. Silverman, in *Proceedings of the 4th International Symposium on Electron and Photon Interactions at High Energies*, Daresbury 1969.

[17] R. Diebold, *Boulder Conf.* 1969 and *SLAC Report.*
[18] E. Lohrmann, *Lund Conf.* 1969 (see Ref. [10]).
[19] See Ref. [8].
[20] L. Bertocchi, *Herceg-Novi School* 1969, Strasbourg—Belgrade.
[21] T. D. Lee, C. S. Wu, *Ann. Rev. Nuclear Sci.*, **16**, 51 (1966).
[22] F. Gilman, *Phys. Rev.*, **171**, 1453 (1968).
[23] *Proceedings of the CERN Conference on Weak Interactions*, 1969, CERN 69–7.
[24] K. Gottfried, D. R. Yennie, *Phys. Rev.*, **182**, 1595 (1969).
[25] Particle Data Group, A. Barbaro-Galtieri *et al.*, *Rev. Mod. Phys.*, **42**, 87 (1970).
[26] J. F. Allard *et al.*, *Phys. Letters*, **19**, 431 (1965); **12**, 143 (1964); *Nuovo Cimento*, **46**, 737 (1966).
[27] A. M. Cnops *et al.*, *Phys. Rev. Letters*, **25**, 1132 (1970).
[28] See D. R. O. Morrison's talk at the *Lund Conf.* 1969 (see Ref. [10]) for a discussion and references related to this point.
[29] See H. Pilkuhn, *Trieste Conf.* 1970 (see Ref. [1]) for a recent discussion of this possibility and references.
[30] See for example M. Froissart, R. Omnes, in *High Energy Physics*, Les Houches 1965, ed. C. de Witt and M. Jacob, (Gordon and Breach, New York 1965); J. D. Jackson, in *Proceedings of the XIIIth Conference on High Energy Physics*, Berkeley 1966, p. 152, see also Refs [7], [31].
[31] B. Daugeras, *Thèse Université*, Paris-Sud (1971).
[32] M. Abolins *et al.*, *Phys. Rev. Letters*, **15**, 125 (1965).
[33] B. A. Shahbazian, *Nuclear Phys.*, **B1**, 16 (1967).
[34] B. Eisenstein, H. Gordon, *Phys. Rev.*, **1D**, 841 (1970).
[35] A. Forino *et al.*, *Phys. Letters*, **19**, 68 (1965).
[36] R. Vanderhaghen *et al.*, *Nuclear Phys.*, **B13**, 329 (1969).
[37] B. J. Deery *et al.*, *Phys. Letters*, **31B**, 82 (1970).
[38] G. Vegni *et al.*, *Phys. Letters*, **19**, 526 (1965).
[39] G. Bellini *et al.*, *Nuovo Cimento*, **29**, 896 (1963); **40A**, 949 (1965).
[40] M. Firebaugh *et al.*, in *Proceedings of the XVth Conference on High Energy Physics, Kiev Conf.* 1970, *Wisconsin-Toronto preprint*; M. Firebaugh, private communication.
[41] A. M. Cnops *et al.*, *Phys. Rev. Letters*, **21**, 1609 (1968); *Phys. Letters*, **29B**, 45 (1969).
[42] S. Y. Fung, A. Kernan, Y. Oh, R. Poe, T. Schalk, B. C. Shen, University of California Riverside, private communication.
[43] P. Kemp *et al.*, *Kiev Conf.* 1970 (see Ref. [40]), *Durham, Genoa, Milan, Paris preprint.* See also G. Vegni, *Trieste Conf.* 1970 (see Ref. [1]).
[44] M. Banier *et al.*, *Durham, Genoa, Milan, Paris preprint, Amsterdam Conf.* 1971.
[45] K. Paler *et al.*, Purdue Univ., private communication.
[46] C. Bemporad *et al.*, *CERN, ETH, ICL, Milano, Kiev Conf.* 1970 and *Amsterdam Conf.* 1971 *preprints.*
[47] B. Daugeras *et al.*, *Phys Letters*, **27B**, 332 (1968).
[48] F. R. Huson *et al.*, *Phys. Letters*, **28B**, 208 (1968).
[49] J. J. Veillet, *CERN Conf.* 1968 (see Ref. [12]).
[50] F. R. Huson *et al.*, *Phys. Letters*, **20B**, 91 (1966).
[51] F. R. Huson, W. B. Fretter, *Nuovo Cimento*, **33**, 1 (1964).
[52] A. Caforio *et al.*, *Nuovo Cimento*, **32**, 1471 (1964).
[53] E. V. Anzon *et al.*, *Phys. Letters*, **31B**, 241 (1970).
[54] K. Rybicki, *Trieste Conf.* 1970 (see Ref. [1]); See also Refs [53], [66].
[55] Z. Czachowska *et al.*, *Nuovo Cimento*, **49**, 303 (1967).
[56] J. I. Rhode *et al.*, *Phys. Rev.*, **178**, 2089 (1969).
[57] I. Butterworth *et. al.*, *Phys. Rev. Letters*, **15**, 500 (1965).
[58] K. Buchner *et al.*, *Nuclear Phys.*, **B9**, 286 (1969).
[59] N. Hoogland *et al.*, *Nuclear Phys.*, **B11**, 309 (1969).
[60] B. Eisenstein *et al.*, *University of Illinois preprint, Kiev Conf.* 1970, (see Ref. [40]); M. R. Robinson, private communication.

[61] B. Werner *et al.*, *Phys. Rev.*, **188**, 2023 (1969).
[62] A. M. Cnops *et al.*, *Phys. Rev. Letters*, **25** 1132 (1970).
[63] M. Haguenauer *et al.*, *Paris, Bergen, Strasbourg, Madrid preprint, Kiev Conf.* 1970 (see Ref. [40]).
[64] P. Antich, *Kiev Conf.* 1970, *Johns Hopkins Univ. preprint*; D. Denegri *et al.*, *Phys. Rev. Letters*, **20**, 1194 (1968) and Johns Hopkins Univ. *thesis*; D. Denegri *et al.*, *Nuclear Phys.*, **B28**, 13 (1971).
[65] A. Firestone, G. Goldhaber, A. Lissauer, G. Trilling, LRL, Berkeley, private communication.
[66] As quoted by Professor Mięsowicz during this school.
[67] R. L. Eisner *et al.*, *Phys. Letters*, **28B**, 356 (1968).
[68] P. C. Brunt *et al.*, *Phys. Letters*, **26B**, 317 (1968).
[69] H. Braun *et al.*, *Phys. Rev.*, **2D**, 1212 (1970); D. Evrard *et al.*, *Nuclear Phys.*, **B14**, 699 (1969).
[70] F. R. Huson *et al.*, *Nuclear Phys.*, **B8**, 391 (1968).
[71] P. D. O'Brien *et al.*, Michigan-Princeton Collaboration, private communication from Professor L. Jones; C. Zemach, *Phys. Rev.*, **133B**, 1200 (1964).
[72] E. H. de Groot, G. F. Wolters, *Phys. Letters*, **26B**, 636 (1968).
[73] Durham–Geneva–Milano–Paris (EP, IPN) Collaboration, $\pi^+ d$ at 11.7 GeV/c quoted by G. Vegni in *Trieste Conf.* 1970 (see Ref. [1]).
[74] K. Rybicki, *Inst. Nuclear Phys. Cracow, Report* No 694/PH, 1969.
[75] That the d^* is not a resonance is shown by the $\pi^+ d$ "decay" angular distribution, which is sharply peaked implying the presence of a large number of partial waves. The d^* is centered roughly at the sum of the nucleon and Δ (1238) masses and is roughly as wide as the Δ (1238). The d^* is probably due to Δ (1238) formation on one nucleon in the deuteron (along with other particles *e.g.* a ϱ^0 in $\pi^+ d \to \varrho^0 \pi^+ d$), followed by $\Delta \to n\pi$ decay in such a way that this n and the spectator nucleon can recombine to form a recoiling deuteron. See Evrard *et al.*,[69] for a recent discussion, Stodolsky [5] for discussion of collective excitation of low lying nuclear levels of heavier nuclei and von Bochmann and Margolis (*Nuclear Phys.*, **B14**, 609 (1969)) for discussion of other possible two or multistep processes in nuclei.